Am J Physiol Renal Physiol 299: F1004–F1013, 2010.
First published August 25, 2010; doi:10.1152/ajprenal.00587.2009.

Allogenic fetal membrane-derived mesenchymal stem cells contribute to renal repair in experimental glomerulonephritis

Hidetoshi Tsuda,[1,2,3] Kenichi Yamahara,[1] Shin Ishikane,[1] Kentaro Otani,[1] Atsuhiro Nakamura,[1,5] Kazutomo Sawai,[6] Naotsugu Ichimaru,[7] Masaharu Sada,[1] Akihiko Taguchi,[1] Hiroshi Hosoda,[1] Masahiro Tsuji,[1] Hiroshi Kawachi,[8] Masaru Horio,[3] Yoshitaka Isaka,[2] Kenji Kangawa,[6] Shiro Takahara,[2] and Tomoaki Ikeda[1,4]

Departments of [1]Regenerative Medicine and Tissue Engineering and [6]Biochemistry, National Cardiovascular Center Research Institute; Departments of [2]Advanced Technology for Transplantation, [3]Functional Diagnostic Science, Course of Health Science, and [7]Urology, Osaka University Graduate School of Medicine, Suita; [4]Department of Perinatology, National Cardiovascular Center, Osaka; [5]Second Department of Internal Medicine, Nara Medical University, Nara; and [8]Department of Cell Biology, Institute of Nephrology, Niigata University Graduate School of Medical and Dental Sciences, Niigata, Japan

Submitted 14 October 2009; accepted in final form 24 August 2010

Tsuda H, Yamahara K, Ishikane S, Otani K, Nakamura A, Sawai K, Ichimaru N, Sada M, Taguchi A, Hosoda H, Tsuji M, Kawachi H, Horio M, Isaka Y, Kangawa K, Takahara S, Ikeda T. Allogenic fetal membrane-derived mesenchymal stem cells contribute to renal repair in experimental glomerulonephritis. *Am J Physiol Renal Physiol* 299: F1004–F1013, 2010. First published August 25, 2010; doi:10.1152/ajprenal.00587.2009.—Mesenchymal stem cells (MSC) have been reported to be an attractive therapeutic cell source for the treatment of renal diseases. Recently, we reported that transplantation of allogenic fetal membrane-derived MSC (FM-MSC), which are available noninvasively in large amounts, had a therapeutic effect on a hindlimb ischemia model (Ishikane S, Ohnishi S, Yamahara K, Sada M, Harada K, Mishima K, Iwasaki K, Fujiwara M, Kitamura S, Nagaya N, Ikeda T. *Stem Cells* 26: 2625–2633, 2008). Here, we investigated whether allogenic FM-MSC administration could ameliorate renal injury in experimental glomerulonephritis. Lewis rats with anti-Thy1 nephritis intravenously received FM-MSC obtained from major histocompatibility complex-mismatched ACI rats (FM-MSC group) or a PBS (PBS group). Nephritic rats exhibited an increased urinary protein excretion in the PBS group, whereas the FM-MSC group rats had a significantly lower level of increase ($P < 0.05$ vs. PBS group). FM-MSC transplantation significantly reduced activated mesangial cell (MC) proliferation, glomerular monocyte/macrophage infiltration, mesangial matrix accumulation, as well as the glomerular expression of inflammatory or extracellular matrix-related genes including TNF-α, monocyte chemoattractant protein 1 (MCP-1), type I collagen, TGF-β, type 1 plasminogen activator inhibitor (PAI-1) ($P < 0.05$ vs. PBS group). In vitro, FM-MSC-derived conditioned medium significantly attenuated the expression of TNF-α and MCP-1 in rat MC through a prostaglandin E_2-dependent mechanism. These data suggest that transplanted FM-MSC contributed to the healing process in injured kidney tissue by producing paracrine factors. Our results indicate that allogenic FM-MSC transplantation is a potent therapeutic strategy for the treatment of acute glomerulonephritis.

prostaglandin E_2; cell therapy; anti-Thy-1 nephritis

MESENCHYMAL STEM CELLS (MSC) are multipotent stem cells present in bone marrow (BM), adipose tissue, and many other organs and have the ability to differentiate into a variety of lineages including adipocytes, osteocytes, and chondrocytes (9, 11, 42). Previous reports described that BM-derived stem cells including MSC contributed to the repair of several compartments of the kidney, including the endothelium (47), interstitium (16), epithelium (23), and the mesangium (21). Moreover, several studies have demonstrated that transplanted BM-derived MSC (BM-MSC) contribute to improve renal function in experimental glomerulonephritis induced by anti-Thy1 (31, 58). These features make BM-MSC an attractive therapeutic tool for the treatment of renal diseases.

However, there are limitations in using autologous BM-MSC as a source of regenerative medicine. BM aspiration may be painful and sometimes yields low numbers of MSC on processing (61). Therefore, an alternative source of MSC that can be obtained noninvasively and in large quantities would be advantageous. Fetal membrane (FM), which is generally discarded as medical waste, has been found to be a rich, easily expandable source of MSC (18, 43). Recently, we demonstrated that transplantation of allogenic FM-derived MSC (FM-MSC) as well as autologous BM-MSC induced therapeutic angiogenesis using a rat hindlimb ischemia model (20). These results suggest that allogenic FM-MSC are a potential alternative to autologous BM-MSC as a source of regenerative therapy.

In the present study, we investigated whether systemic administration of allogenic FM-MSC could improve the course of anti-Thy1 nephritis. Anti-Thy1 nephritis is a model of mesangioproliferative glomerulonephritis characterized by mesangiolysis followed by repair via mesangial cell (MC) proliferation, mesangial matrix accumulation, and monocyte/macrophage influx (25). Because we previously reported that MSC possessed paracrine angiogenic and anti-fibrotic effects (20, 39), we also examined the contribution of the paracrine effects to ameliorate anti-Thy1 nephritis after allogenic FM-MSC transplantation.

MATERIALS AND METHODS

Animals. All experimental protocols were approved by the Animal Care Committee of the National Cardiovascular Center Research Institute. Different strains of rats were used according to their major histocompatibility complex (MHC) antigen disparity: Lewis (MHC haplotype: RT-1l) and ACI (MHC haplotype: RT-1a) rats (Japan SLC, Hamamatsu, Japan). Green fluorescent protein

Address for reprint requests and other correspondence: K. Yamahara, Dept. of Regenerative Medicine and Tissue Engineering, National Cardiovascular Center Research Institute, 5-7-1 Fujishirodai, Suita, Osaka 565-8565, Japan (e-mail: yamahara@ri.ncvc.go.jp).

(GFP)-transgenic Lewis rats (Institute of Laboratory Animals, Kyoto University, Kyoto, Japan) were used to investigate the distribution of injected FM-MSC.

Isolation and expansion of FM-MSC and glomerular MC. Isolation and expansion of FM-MSC were performed as previously described (20). In brief, FM was obtained from pregnant rats on *day 15* postconception. Minced FM was digested with type II collagenase solution (300 U/ml; Worthington Biochemical, Lakewood, NJ) for 1 h at 37°C. After filtration and centrifugation, FM-derived cells were suspended in α-MEM (Invitrogen, Carlsbad, CA) supplemented with 10% fetal bovine serum (FBS; Invitrogen) and 1% penicillin/streptomycin (Invitrogen) and cultured in standard plastic dishes. The adherent MSC populations appeared by *days 5–7*, and these FM-MSC were used for the experiments at *passage 3–6*.

Glomerular MC were established as described elsewhere (29). MC obtained from Sprague-Dawley rats were cultured in standard medium (DMEM, high glucose, Invitrogen, 10% FBS, and 1% penicillin/streptomycin) and used for experiments at *passages 13–15*.

Experimental model and design. Mesangial proliferative glomerulonephritis was induced in 6-wk-old male Lewis rats (170–180 g) by intravenous injection of anti-Thy1 monoclonal antibody (mAb 1–22-3; 0.5 mg/rat) (24). Because FM-MSC reportedly express high levels of Thy1 (20), we administered FM-MSC on *day 2* after anti-Thy1 antibody injection when its antibody in plasma is undetectable (Supplemental Figure and Method; supplemental material for this article is available online at the journal website). On *day 2* after mAb injection, rats were randomized to two groups: *1*) FM-MSC injection (FM-MSC group; $n = 8$) and *2*) control PBS injection alone (PBS group; $n = 8$). A total of 5×10^5 FM-MSC obtained from MHC mismatched ACI rats or PBS (200 μl each) was injected into the tail vein of Lewis nephritic rats. Sham rats (Sham group; $n = 8$) received a PBS injection instead of mAb. On *days 7* and *14*, rats were placed in metabolic cages for collection of urine to determine the excretion of urine protein.

Histological examination. Kidney tissues were fixed with 4% phosphate-buffered formalin solution (Wako Pure Chemical Industries, Osaka, Japan), embedded in paraffin block, and cut into 2-μm sections. To quantify mesangial matrix accumulation, sections were stained with periodic acid-Schiff (PAS), photographed using a digital microscope (BIOREVO BZ-9000; KEYENCE, Osaka, Japan), and evaluated by assessing 30 randomly selected glomeruli/kidney and scoring each glomerulus on a semiquantitative scale (0–4) as described previously (19).

Immunohistochemical staining was performed with mouseanti-α-smooth muscle actin (α-SMA) antibody (clone 1A4; Dako, Glostrup, Denmark), mouse anti-CD68 antibody (clone ED-1; Serotec, Oxford, UK), and rabbit anti-GFP antibody (Invitrogen). Negative control staining was performed by replacing the primary antibody with normal IgG. Following antigen retrieval, endogenous peroxidase activity was quenched with 1.5% H_2O_2 for 10 min. The first antibodies were incubated for 1 h at room temperature, followed by incubation with Envision system-horseradish peroxidase-labeled polymer (Dako) for 30 min. The sections were visualized with 3,3′diaminobenzidine tetrahydrochloride (Dako) and counterstained with hematoxylin.

The α-SMA-positive area relative to the glomerular area was calculated as a percentage using a computer-aided manipulator (WinRoof; Mitani, Fukui, Japan). The α-SMA staining percentage of total glomerular area was determined, and the mean value of 30 randomly selected glomeruli was calculated. The number of ED-1-positive monocytes/macrophages was evaluated by counting stained cells per glomerulus in at least 30 randomly selected glomeruli. To evaluate the distribution of GFP-positive administered cells, we counted all the GFP-positive cells in one randomly selected section ($n = 4$) from each organ and an overall average for all rats was calculated.

Quantitative RT-PCR analysis. Glomeruli were isolated from rat kidneys using a graded sieving technique (19). Total RNA was extracted from isolated glomeruli using an RNeasy mini kit (Qiagen, Hilden, Germany). Obtained RNA was reverse-transcribed into cDNA using a Quantitect Reverse Transcription kit (Qiagen). PCR amplification was performed using Power SYBR Green PCR Master Mix (Applied Biosystems, Foster City, CA). β-Actin transcript was used as an internal control. Primers used are listed in Table 1.

Western blot analysis. Western blotting was performed as previously described (36). Briefly, kidney tissues were homogenized in 0.1% Tween 20 with a protease inhibitor, loaded (30 μg) on a 10–20% gradient gel (Bio-Rad, Hercules, CA), and blotted onto a polyvinylidene difluoride membrane (Millipore, Bedford, MA). After blocking for 1 h, membranes were incubated with mouse anti-monocyte chemoattractant protein (MCP)-1 antibody (1:1,000; BD Biosciences Pharmingen, San Jose, CA), then incubated with peroxidase-labeled secondary antibody (1:1,000; Cell Signaling Technology, Danvers, MA). Positive protein bands were visualized with an ECL kit (GE Healthcare, Piscataway, NJ) and measured by densitometry. A mouse monoclonal antibody against β-actin (Sigma-Aldrich, St. Louis, MO) was used as a control ($n = 8$ in each group).

Assessment of paracrine effects of FM-MSC on glomerular MC. Conditioned medium was collected from 1×10^6 cells of FM-MSC cultured in 8 ml of standard medium (DMEM supplemented with 10% FBS and 1% penicillin/streptomycin) with or without the cyclooxygenase (COX) 2 inhibitor NS-398 (0.1 μM; Wako) for 48 h, and filtered through a 0.22-μm filtration unit (Millipore). MC were plated on six-well plates (2×10^5 cells/well) with standard medium for 24 h. The medium was then changed to serum-free DMEM for 24 h, followed by conditioned medium obtained from FM-MSC. After 8 h, total RNA was extracted from MC.

ELISA. The concentration of PGE_2 in the conditioned medium of FM-MSC was determined using an ELISA kit, according to the

Table 1. *Primers for qRT-PCR*

Gene	Forward	Reverse
Type I collagen	5′-AATGGTGCTCCTGGTATTGC-3′	5′-GGTTCACCACTGTTGCCTTT-3′
TGF-β	5′-CTACTGCTTCAGCTCCACAGAGA-3′	5′-ACCTTGGGCTTGCGACC-3′
PAI-1	5′-ACCTCGATCTTGACCTTTTG-3′	5′-GACAATGGAAGAGCAACATG-3′
MMP-2	5′-GATCTGCAAGCAAGACATTGTCTT-3′	5′-GCCAAATAAACCGATCCTTGAA-3′
MMP-9	5′-TGGAACTCACACAACGTCTTTCA-3′	5′-TCACCCGGTTGTGGAAACTC-3′
TIMP-1	5′-ATCAAGATGACTAAGATGCTCAAAGG-3′	5′-GGCCCGCGATGAGAAACT-3′
TNF-α	5′-TGCCTCAGCCTCTTCTCATT-3′	5′-CCCATTTGGGAACTTCTCCT-3′
MCP-1	5′-ATGCAGGTCTCTGTCACGCT-3	5′-GGTGCTGAAGTCCTTAGGGT-3′
HGF	5′-TGCAACGGTGAAAGCTACAG-3′	5′-AGCCCTTGGTCGGGATATCTT-3′
VEGF	5′-AGAAAGCCCAATGAAGTGGTG-3′	5′-ACTCCAGGGCTTCATCATTG-3′
β-Actin	5′-GCCCTAGACTTCGAGC-3′	5′-CTTTACGGATGTCAACGT-3′

TGF, transforming growth factor; PAI-1, type 1 plasminogen activator inhibitor; MMP, membrane-type matrix metalloproteinase; TIMP-1, tissue inhibitor of MMP-1; MCP-1, monocyte chemoattractant protein 1.

manufacturer's protocol (Cayman Chemical, Ann Arbor, MI). The absorbance was measured by a microplate reader (Bio-Rad) at 405 nm.

Statistical analysis. All data are expressed as means ± SE. Comparisons between two parameters were analyzed by using the unpaired Student's *t*-test. Comparisons of parameters among the three groups were made by one-way ANOVA, followed by Tukey's test. A value of $P < 0.05$ was considered statistically significant.

RESULTS

Reduction of proteinuria by FM-MSC transplantation. In the anti-Thy1 nephritic model, transient renal damage with massive proteinuria developed (25). On *day 7*, the 24-h urine protein excretion rate was significantly increased in rats with anti-Thy1 nephritis (84.9 ± 7.6 mg/24 h in the PBS group) compared with control (10.7 ± 0.5 mg/24 h in the Sham group), and FM-MSC treatment significantly reduced this increase (60.8 ± 8.0 mg/24 h, $P < 0.05$ vs. PBS group) (Fig. 1). On *day 14*, the 24-h urine protein excretion rate in these three groups fell to within the normal range. Creatinine clearance was significantly decreased in nephritic rats (2.14 ± 0.06 ml/min in the PBS group) compared with the Sham group (2.97 ± 0.15 ml/min, $P < 0.01$). However, no significant difference in creatinine clearance was observed between the PBS and FM-MSC groups (2.14 ± 0.09 ml/min in the FM-MSC group).

Inhibition of accumulation of activated MC and mesangial matrix by FM-MSC transplantation. Glomerular expression of α-SMA, a marker of activated MC, was increased after disease induction (Fig. 2, *D–F*). Expression of α-SMA in nephritic rats increased to a peak level on *day 7* and then gradually decreased thereafter (Fig. 2*M*). On *days 7* and *14*, α-SMA staining of the glomerular area in FM-MSC-treated rats (30.7 ± 0.8 and 22.4 ± 0.8%, respectively) was significantly decreased compared with the PBS group (37.5 ± 0.6 and 26.6 ± 0.7%, respectively, $P < 0.01$ vs. FM-MSC group).

PAS staining in rats with anti-Thy1 nephritis revealed the accumulation of mesangial matrix (Fig. 2, *G–I*). Similar to α-SMA expression, the glomerular PAS-positive area in nephritic rats reached its peak on *day 7* (PAS score; 2.72 ± 0.12 in the PBS group vs. 0.20 ± 0.05 in the Sham group, $P < 0.01$) and remained elevated on *day 14* (2.97 ± 0.08 in the PBS group and 0.25 ± 0.05 in the Sham group, $P < 0.01$), which was significantly decreased by FM-MSC administration (FM-MSC group: 2.21 ± 0.08 on *day 7* and 1.54 ± 0.06 on *day 14*, $P < 0.05$ vs. PBS group) (Fig. 2*N*). qRT-PCR analysis revealed that the reduction of mesangial matrix accumulation in FM-MSC-treated rats was associated with decreased expression of glomerular type I collagen, transforming growth factor (TGF) -β, type 1 plasminogen activator inhibitor (PAI-1) ($P < 0.05$ vs. PBS group) (Fig. 3, *A–C*). However, FM-MSC treatment did not significantly affect the glomerular expression of membrane-type matrix metalloproteinases (MMPs) and tissue inhibitor of MMP-1 (TIMP-1) in anti-Thy1 nephritic rats (Fig. 3, *D–F*).

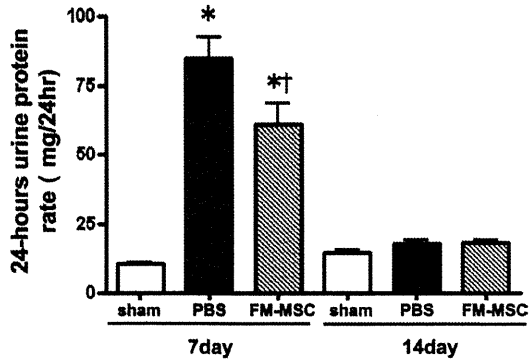

Fig. 1. Effect of fetal membrane-derived mesenchymal stem cells (FM-MSC) administration on proteinuria in anti-Thy1 nephritis. The 24-h urine protein excretion rate was measured in the Sham, PBS, and FM-MSC groups. On *day 7*, the rate was significantly increased in the PBS group compared with the FM-MSC group. On *day 14*, both groups showed remission of proteinuria, and no significant differences were seen among these 3 groups. *$P < 0.05$ vs. Sham group. †$P < 0.05$ vs. PBS group.

Attenuation of glomerular monocyte/macrophage influx by FM-MSC transplantation. Immunostaining of ED-1 in rats with anti-Thy1 nephritis revealed a significant monocyte/macrophage infiltration into the glomeruli (Fig. 2, *J–L*). On *day 7*, the number of infiltrating monocytes/macrophages in the PBS group (7.5 ± 0.2/glomerulus) was significantly higher than in the Sham group (0.4 ± 0.1/glomerulus), which was significantly lower than in the FM-MSC group (6.0 ± 0.2/glomerulus, $P < 0.01$ vs. PBS group) (Fig. 2*O*). A similar result was also observed on *day 14* (PBS group 5.1 ± 0.2/glomerulus vs. FM-MSC group 3.9 ± 0.1/glomerulus, $P < 0.01$).

Reduction of renal inflammatory cytokine/chemokine expression by FM-MSC transplantation. We examined the glomerular expression of inflammatory cytokines/chemokines in nephritic rats on *day 7*. QRT-PCR analysis showed that tumor necrosis factor (TNF)-α expression in glomeruli was significantly increased by 7.70 ± 0.54-fold in the PBS group ($P < 0.01$ vs. the Sham group), and this increase was significantly decreased in the FM-MSC group (5.92 ± 0.20-fold, $P < 0.05$ vs. PBS group) (Fig. 3*G*). Glomerular MCP-1 mRNA expression in the PBS group showed a 5.41 ± 0.38-fold increase compared with the Sham group ($P < 0.01$) (Fig. 3*H*), but FM-MSC transplantation reduced this increase by >30% (3.51 ± 0.51-fold, $P < 0.05$ vs. PBS group). Similarly, Western blot analysis showed that renal MCP-1 protein expression in the PBS group was significantly increased compared with the Sham group (7.65 ± 2.49-fold, $P < 0.05$) (Fig. 4), and FM-MSC administration showed a tendency of decreasing the expression of MCP-1 protein (6.44 ± 0.96-fold vs. the Sham group) (Fig. 4).

Renal expression of VEGF and HGF after FM-MSC transplantation. Previously, we reported that cultured FM-MSC secreted large amounts of angiogenic/antiapoptotic factors including VEGF and HGF (20). Because VEGF and HGF have been reported as renoprotective factors (34, 41, 53, 55), we analyzed glomerular expression of these factors in FM-MSC-transplanted nephritic rats. qRT-PCR analysis revealed that expression of VEGF mRNA in the PBS group was significantly decreased (0.36 ± 0.07-fold vs. Sham group, $P < 0.05$), and no significant upregulation was seen after FM-MSC administration (0.30 ± 0.08-fold vs. Sham group, $P < 0.05$) (Fig. 3*I*). Glomerular expression of HGF mRNA was significantly increased in the PBS group (2.64 ± 0.38-fold vs. Sham group, $P < 0.05$), but no significant difference was observed between PBS and FM-MSC groups (2.51 ± 0.34-fold vs. Sham group, $P < 0.05$) (Fig. 3*J*).

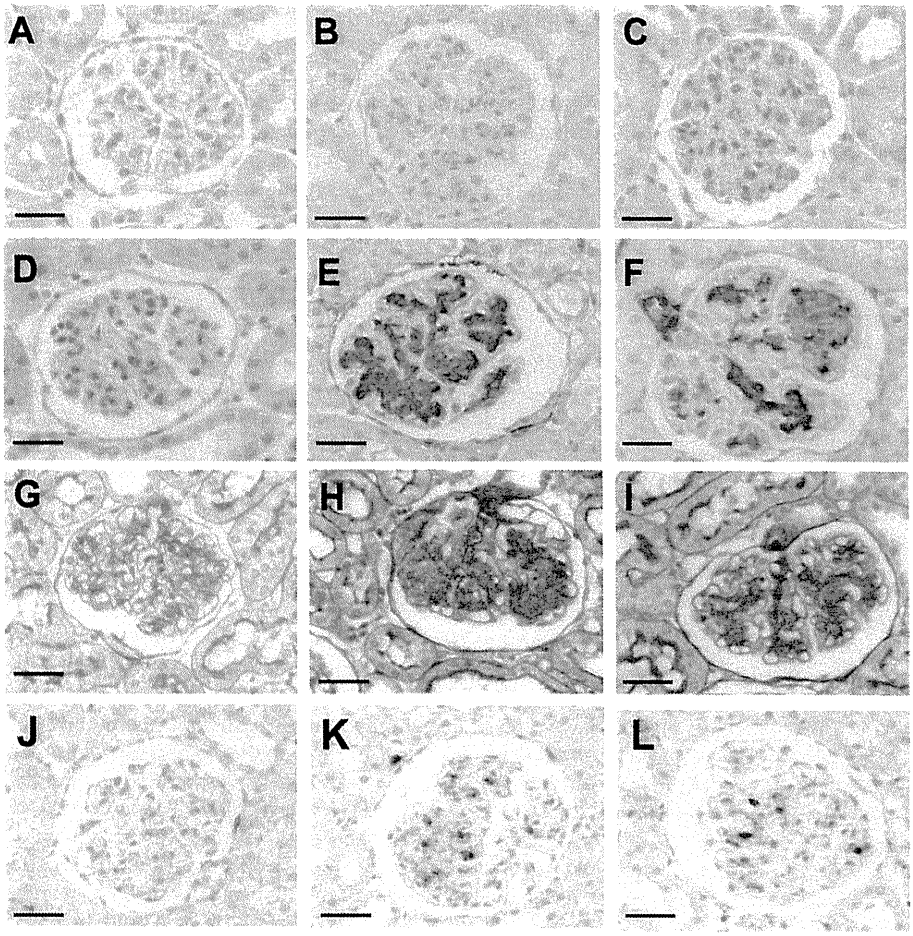

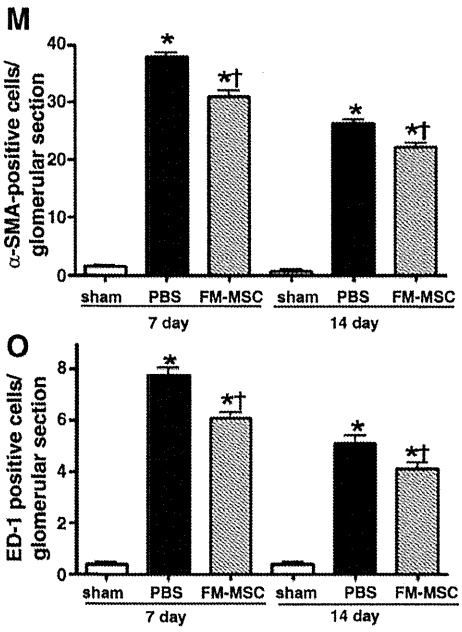

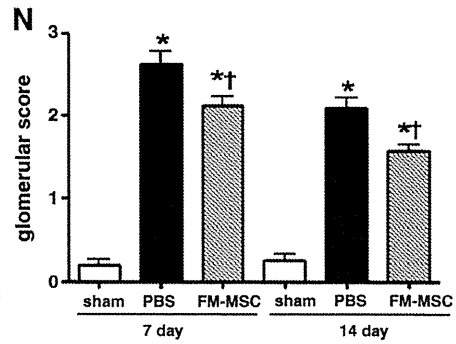

Fig. 2. Inhibition of the accumulation of activated MC, mesangial matrix, and glomerular monocyte/macrophages by FM-MSC transplantation in rats with anti-Thy1 nephritis. *A–L*: representative micrographs of negative control (*A–C*), α-smooth muscle actin (SMA; *D–F*), periodic acid-Schiff (PAS; *G–I*) and ED-1 (*J–L*) staining in the Sham (*A*, *D*, *G*, *J*), PBS (*B*, *E*, *H*, *K*) and FM-MSC (*C*, *F*, *I*, *L*) groups on *day 7*. *M*: quantitative analysis revealed that the number of α-SMA-positive activated MC was lower in the FM-MSC group compared with the PBS group on *days 7* and *14*. *N*: mesangial matrix accumulation was significantly reduced in the FM-MSC group compared with the PBS group on *days 7* and *14*. *O*: the number of infiltrated ED-1-positive monocytes/macrophages was significantly reduced in the FM-MSC group compared with the PBS group on *days 7* and *14*. Scale bars = 20 μm. $*P < 0.05$ vs. Sham. $\dagger P < 0.05$ vs. PBS group.

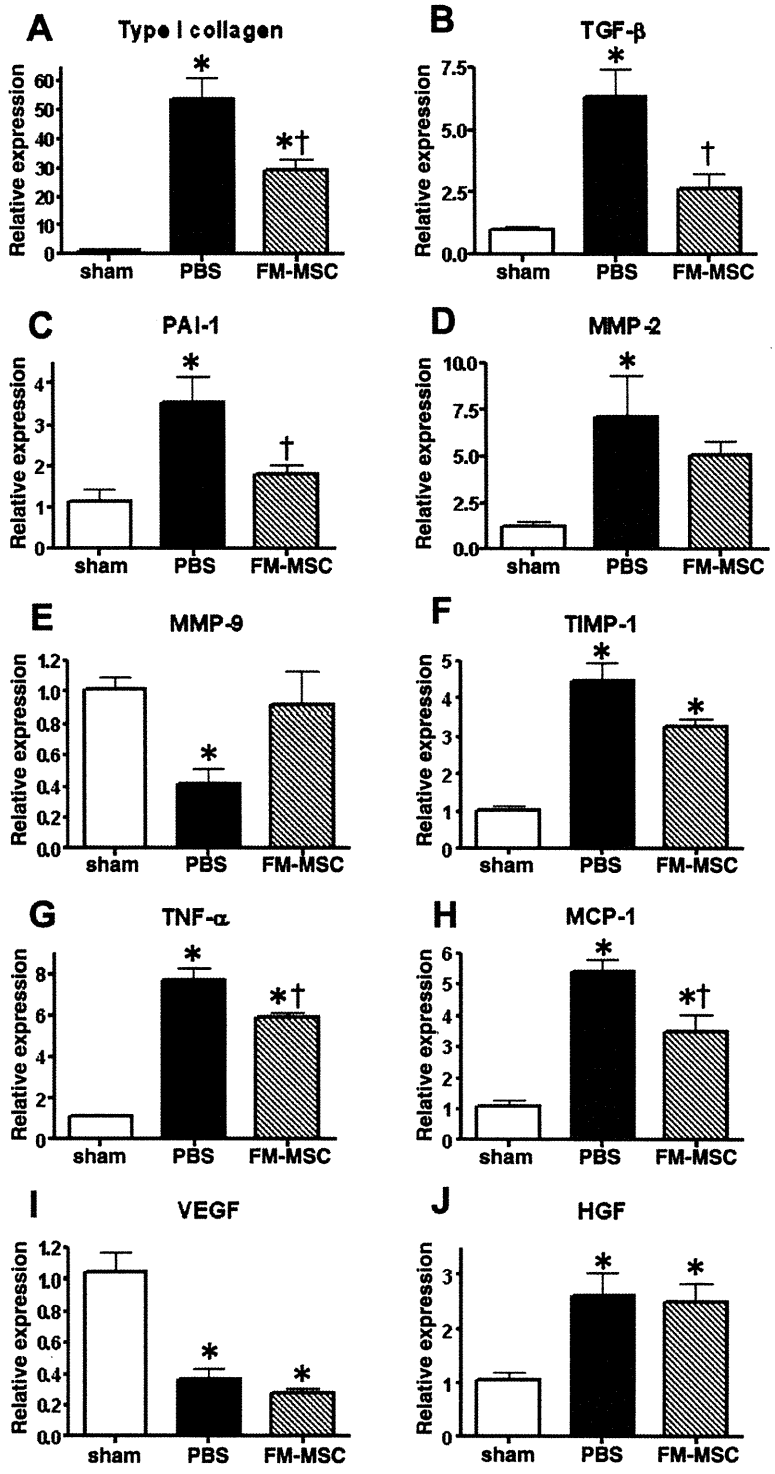

Fig. 3. Quantitative RT-PCR analysis of extracellular matrix, inflammatory-, and angiogenesis-related genes in the kidney of rats with anti-Thy1 nephritis and FM-MSC administration. Expression of mRNA for type I collagen (*A*), transforming growth factor (TGF)-β (*B*), type 1 plasminogen activator inhibitor (PAI-1; *C*), TNF-α (*G*), and monocyte chemoattractant protein (MCP-1; *H*) in glomeruli was markedly increased in anti-Thy1 nephritic rats on *day 7*, which was significantly attenuated in FM-MSC-transplanted rats. No significant difference in mRNA expression of membrane-type matrix metalloproteinase 2 (MMP-2; *D*), MMP-9 (*E*), tissue inhibitor of MMP-1 (TIMP-1; *F*), VEGF (*I*), and HGF (*J*) was seen between the PBS and FM-MSC groups. (n = 8/group). *$P < 0.05$ vs. Sham group. †$P < 0.05$ vs. PBS group.

Engraftment of intravenously injected FM-MSC in rats with anti-Thy1 nephritis. To investigate the behavior of intravenously administered FM-MSC in anti-Thy1 nephritic rats, FM-MSC derived from GFP transgenic Lewis rats were intravenously administered into allogenic ACI rats on *day 2* after mAb injection (n = 4). Twenty-four hours after FM-MSC transplantation, several GFP-positive cells were detected in the kidney sections (12.7 ± 0.3 cells/cm^2) including glomeruli (Fig. 5*A*), proximal tubule (Fig. 5*B*), and interstitial area (Fig. 5*C*). We also detected GFP-positive FM-MSC in sections of lung (Fig. 5*D*), liver (Fig. 5*E*), and spleen (Fig. 5*F*). A significant number of GFP-positive FM-MSC were seen in the

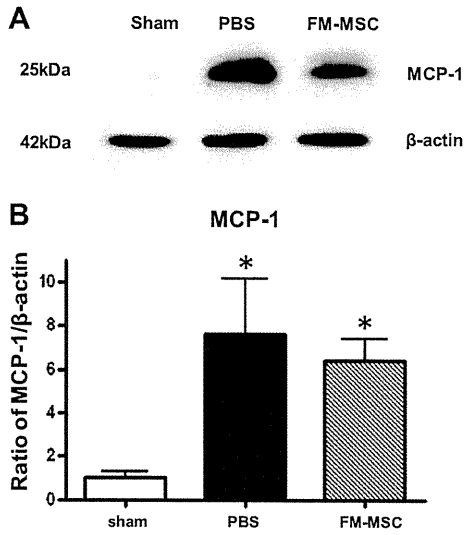

Fig. 4. Decreased MCP-1 protein expression in the renal tissue of nephritic rats after FM-MSC administration. *A*: representative Western blot analysis of MCP-1 in the Sham, PBS, and FM-MSC groups. *B*: quantitative analysis of immunoreactive bands for MCP-1 demonstrated that MCP-1 protein expression in the PBS group was significantly upregulated compared with the Sham group ($P < 0.05$, $n = 8$), and FM-MSC administration showed a tendency toward decreased expression.

lung (119.2 ± 5.1 cells/cm^2), and a similar distribution of GFP-positive cells were observed in the liver and spleen (38.4 ± 1.5 and 32.1 ± 2.9 cells/cm^2, respectively). Although no GFP-positive cell was found in the kidney at 7 days after systemic injection of GFP-positive FM-MSC, several GFP-expressing cells were detected in sections of lung, liver, and spleen (37.6 ± 3.1, 26.1 ± 2.7, and 4.8 ± 0.3 cells/cm^2, respectively).

Anti-inflammatory effect of FM-MSC-conditioned medium on cultured MC. Next, we examined whether FM-MSC possess direct anti-inflammatory effects on MC. When MC were cultured in standard medium, gene expression of TNF-α showed a peak at 8 h and then decreased (n = 3–12, Table 2). FM-MSC-conditioned medium induced a significant (>50%) decrease in TNF-α expression after incubation for 8 h ($P <$ 0.05 vs. standard medium) (Table 2). MCP-1 expression in cultured MC showed a peak at 4 h and then decreased (Table 2). Between FM-MSC-conditioned and standard medium, a significant reduction in MCP-1 expression was seen at 4 (>20%) and 8 (>70%) h ($P < 0.05$ vs. standard medium).

Because recent reports have shown that PGE_2 is one of the key modulators for the MSC-induced anti-inflammatory response, PGE_2-depleted conditioned medium of FM-MSC was prepared by treatment with NS-398, a selective inhibitor of COX2 activity (38). ELISA revealed that a significant amount of PGE_2 was detected in FM-MSC-conditioned medium (888.1 ± 123.3 pg/ml), and NS-398 treatment significantly suppressed its production (23.2 ± 2.4 pg/ml, $P < 0.01$). After incubation for 8 h, conditioned medium of NS-389-treated FM-MSC markedly abolished the decreased expression of TNF-α and MCP-1 in rat MC (1.19 ± 0.12- and 0.82 ± 0.06-fold, respectively) (Fig. 6).

DISCUSSION

In this study, we demonstrated that *1*) intravenous injection of allogenic FM-MSC improved disease manifestations in rats with anti-Thy1 glomerulonephritis; *2*) allogenic FM-MSC administration suppressed MC proliferation, glomerular monocyte/macrophage infiltration, mesangial matrix accumulation, and the glomerular expression of inflammatory and extracellular matrix-related molecules in anti-Thy1 nephritis; and *3*) FM-MSC-conditioned medium attenuated the expression of these inflammatory cytokines/chemokines in cultured MC through a PGE_2-dependent mechanism. Therefore, our data indicate that allogenic FM-MSC transplantation would be a potent therapeutic strategy for the treatment of acute glomerulonephritis.

MSC are considered to be an attractive cell source for application in regenerative medicine because of their excellent capacities in proliferation and differentiation (8, 33, 35, 62). MSC are present in various tissues, but the most characterized population is BM-MSC (9, 11, 42). Therefore, the potential of MSC for renal repair has been investigated using BM-MSC (17, 30–32, 54, 56). To consider the clinical setting, donor BM is a suitable source of MSC, because MSC are relatively easy to obtain from BM aspirates and autologous donor MSC are unlikely to be immunologically rejected. However, autologous MSC transplantation is difficult to attempt on acute glomerulonephritis patients, because of a cell-preparatory period and cell transplantation timing. Therefore, allogenic MSC transplantation has more practical therapeutic value in clinical medicine. We have previously characterized a population of MSC from FM tissue, which possesses great advantages due to its abundance, easy accessibility, and angiogenic activity (20). In this study, we demonstrated that intravenous injection of allogenic FM-MSC, similar to reported autologous BM-MSC (31, 58), provided significant improvement in rats with anti-Thy1 nephritis, indicating that allogenic FM-MSC have potential as a source for regenerative-based therapy for glomerulonephritis.

In this study, we demonstrated that allogenic ACI-derived FM-MSC have a therapeutic effect in MHC-mismatched Lewis rats with anti-Thy1 nephritis. FM is known to play a role in preventing rejection of the fetus and is thought to have low immunogenicity (2, 3, 59). MSC have been reported to fail to trigger allogenic T cell proliferation and induce immune tolerance (1, 6). Indeed, we previously demonstrated that FM-MSC expressed surface antigens similar to those of BM-MSC. For example, both types of MSC are negative for MHC II (19). We also confirmed that FM-MSC did not provoke alloreactive lymphocyte proliferation in mixed lymphocyte culture (20). A recent report described that intravenous injection of BM-MSC induced recovery from anti-Thy1 nephritis in outbred allogenic as well as inbred autologous settings (31). These results suggest that FM-MSC as well as BM-MSC could evade T lymphocyte alloreactivity and would be successfully transplantable across MHC barriers.

Several studies have shown beneficial effects of BM-MSC transplantation in renal diseases (17, 30–32, 54, 56). However, the mechanisms underlying the benefit of MSC transplantation remain controversial. One possible mechanism is the differentiation into renal cells of injected MSC. Intravenously administered MSC have been shown to con-

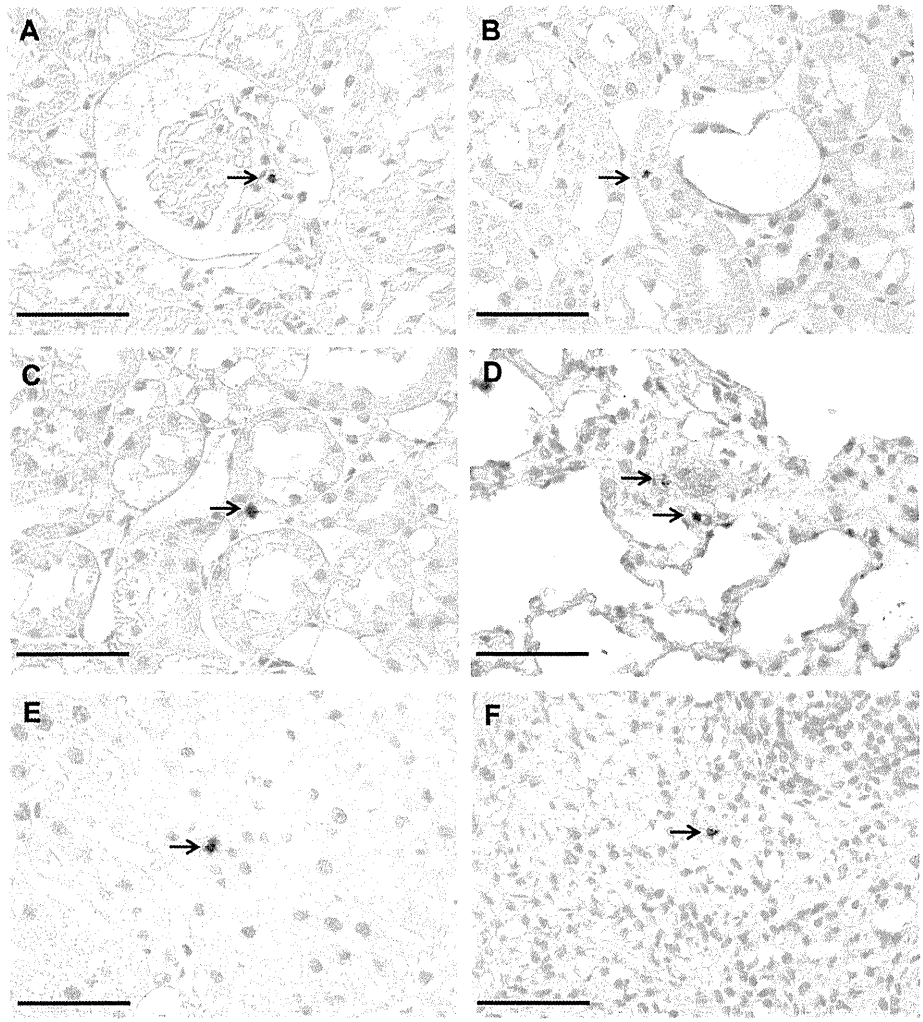

Fig. 5. Engraftment of intravenously injected FM-MSC in rats with anti-Thy1 nephritis. The presence of intravenously injected green fluorescent protein (GFP)-positive FM-MSC was observed 24 h after cell injection (n = 4). *A–F*: representative GFP immunohistochemical staining shows GFP-positive transplanted FM-MSC were found in glomeruli (*A*), proximal tubule (*B*), and renal interstitial tissue (*C*) as well as the lung (*D*), liver (*E*), and spleen (*F*; black arrows). Scale bars = 50 μm.

tribute, via differentiation and engraftment, to the cells of many organs, including the kidney (17, 23, 45, 47). In this study, however, we confirmed that these engraftments were low-frequency events that cannot explain the prompt regenerative responses MSC elicit in damaged kidneys. Using the same anti-Thy1 nephritis model, Kunter et al. (31) reported that they failed to detect any evidence of transdifferentiation of MSC into renal cells. This evidence suggests that the direct contribution of transplanted MSC to tissue regeneration is minimal.

Another possibility explaining how transplanted MSC mediate the protective and regenerative effects in damaged kidney tissue is paracrine action (31, 56, 58). Our previous studies found that FM- and BM-MSC secreted VEGF and HGF, which are well-known potent angiogenic and anti-apoptotic factors that elicited angiogenesis in a hindlimb ischemia model (20). In experimental ischemic acute kidney injury or glomerulonephritis, VEGF or HGF secreted from MSC exerted beneficial effects (31, 46, 56, 58). Based on these results, we examined the glomerular expression of these regenerative factors in anti-Thy1 nephritic rats. Contrary to our expectation, however, no significant induction of VEGF or HGF expression in the kidney was seen after FM-MSC transplantation. Therefore, contribution of these FM-MSC-derived growth factors might be minimal in the repair process of anti-Thy1 nephritis.

Table 2. *Time course of TNF-α and MCP-1 mRNA levels in MC after incubation with standard or FM-MSC-conditioned medium*

	TNF-α			MCP-1		
	4 h	8 h	12 h	4 h	8 h	12 h
Standard medium	100.0 ± 22.4%	155.5 ± 28.5%	154.3 ± 23.2%	100.0 ± 14.7%	20.2 ± 1.7%	26.9 ± 2.9%
FM-MSC-conditioned medium	64.6 ± 19.7%*	83.4 ± 10.6%*	154.4 ± 61.6%	19.9 ± 11.5%*	14.4 ± 1.9%*	31.9 ± 6.7%

MC, mesangial cells; FM-MSC, fetal membrane-derived mesangial stem cells. *$P < 0.05$ vs. standard medium.

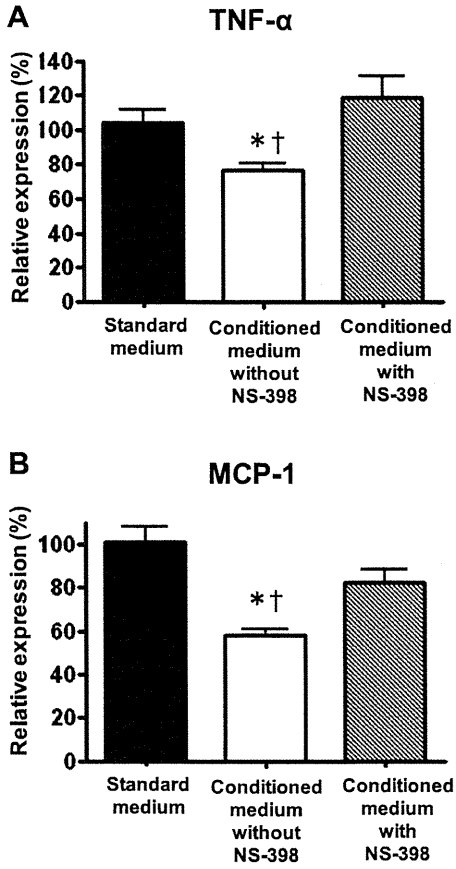

Fig. 6. Effect of FM-MSC-conditioned medium on TNF-α and MCP-1 gene expression in cultured MC. Quantitative RT-PCR analysis in MC after 8 h in culture revealed that TNF-α (*A*) and MCP-1 (*B*) expression was significantly reduced when MC were cultured in FM-MSC-conditioned medium, and this decrease was significantly abolished by the treatment with NS-398 (0.1 μM; $n = 6–12$). *$P < 0.05$ vs. standard medium.

Recently, MSC have been demonstrated to possess immunomodulatory properties (12–14, 22, 27, 28, 37, 49, 51, 52). They are able to modulate the function of lymphocytes (12–14, 22, 28), dendritic cells (37, 49), natural killers (27, 51, 52), and macrophages (26, 38). Several in vivo studies have shown that MSC administration could downregulate the systemic and local inflammatory responses and prevent tissue damage in inflammatory models (4, 15, 63). Therefore, FM-MSC injection might act by modulating the inflammatory responses after the induction of anti-Thy1 nephritis. We previously demonstrated that MSC transplantation attenuated myocardial inflammation in an acute myocarditis model associated with an increase in MCP-1 as well as infiltration of macrophages (40). In the present study, we confirmed that glomerular expression of TNF-α and MCP-1 and macrophage infiltration was significantly suppressed by the administration of FM-MSC. In glomerulonephritis, these inflammatory cytokines/chemokines participate in the activation and accumulation of macrophages, and their infiltration is strongly associated with proteinuria and declining renal function (10, 44, 48, 60).

Recent reports demonstrate that MSC-mediated immunosuppression is mediated by direct contact with immunomodulatory cells including T cells, NK cells, and macrophages, followed by paracrine action of secreted PGE_2 and TGF-β (13, 27, 38). Because intravenously administered FM-MSC survived in kidney, lung, and reticuloendothelial organs including the spleen and liver, these transplanted FM-MSC might change the activity of immunomodulatory cells in nephritic rats by direct contact and paracrine action, which would reduce the inflammatory state of anti-Thy1 nephritis. Previous studies demonstrate that PGE_2 is one of the leading candidates for MSC-induced immune suppression (38). In this study, we confirmed that FM-MSC-conditioned medium contained a significant amount of PGE_2, which was completely depleted by treatment with the COX2 inhibitor NS-398. Gene expression of MCP-1 and TNF-α in MC was decreased by FM-MSC-conditioned media, and this decrease was significantly restored by the treatment with NS-398. A previous report demonstrated that PGE_2 suppressed cytokine/chemokine expression including TNF-α and MCP-1 in MC, which would relate to its anti-inflammatory activity (50). Therefore, PGE_2 would be one of the candidate factors to cause the downregulation of TNF-α and MCP-1 in FM-MSC-treated rats with anti-Thy1 nephritis. Together, previous studies including our own support the hypothesis that paracrine/endocrine actions are of major importance in mediating the protective and regenerative effect of administered MSC after tissue damage.

We have recently reported that MSC transplantation improved cardiac function through an antifibrotic effect in a rat model of dilated cardiomyopathy and acute myocarditis (36, 40) and also demonstrated that the highly expressed genes in cultured MSC included a number of molecules involved in the biogenesis of extracellular matrix (39). These results suggest that transplanted MSC inhibit the fibrogenic process through paracrine actions. In this study, we confirmed that FM-MSC transplantation in anti-Thy1 nephritic rats resulted in reduced mesangial matrix accumulation. In addition, the glomerular expression of several genes involved in fibrogenesis including type I collagen, TGF-β, and PAI-1 was significantly decreased in the FM-MSC group compared with the PBS group. These results support our hypothesis that transplanted MSC possesses antifibrotic activity. However, because the expression of type I collagen, TGF-β, and PAI-1 is associated with renal disease severity (5, 7, 57), decreased expression of these fibrogenic genes in the FM-MSC group might only reflect the degree of renal damage; the precise mechanism by which transplanted FM-MSC prevent renal fibrosis in anti-Thy1 nephritis remains to be elucidated.

In conclusion, our observation that FM-MSC transplantation helped recovery from anti-Thy1 nephritis demonstrates the renoprotective effect of FM-MSC. Because FM-MSC is available non-invasively in large amounts, we suggest that cultured, banked FM-MSC could provide a new therapeutic strategy for the treatment of kidney injury.

DISCLOSURES

No conflicts of interest, financial or otherwise, are declared by the authors.

REFERENCES

1. **Aggarwal S, Pittenger MF.** Human mesenchymal stem cells modulate allogeneic immune cell responses. *Blood* 105: 1815–1822, 2005.
2. **Akle CA, Adinolfi M, Welsh KI, Leibowitz S, McColl I.** Immunogenicity of human amniotic epithelial cells after transplantation into volunteers. *Lancet* 2: 1003–1005, 1981.
3. **Alviano F, Fossati V, Marchionni C, Arpinati M, Bonsi L, Franchina M, Lanzoni G, Cantoni S, Cavallini C, Bianchi F, Tazzari PL, Pasquinelli G, Foroni L, Ventura C, Grossi A, Bagnara GP.** Term amniotic membrane is a high throughput source for multipotent mesenchymal stem cells with the ability to differentiate into endothelial cells in vitro. *BMC Dev Biol* 7: 11, 2007.
4. **Augello A, Tasso R, Negrini SM, Cancedda R, Pennesi G.** Cell therapy using allogeneic bone marrow mesenchymal stem cells prevents tissue damage in collagen-induced arthritis. *Arthritis Rheum* 56: 1175–1186, 2007.
5. **Barnes JL, Mitchell RJ, Torres ES.** Expression of plasminogen activator-inhibitor-1 (PAI-1) during cellular remodeling in proliferative glomerulonephritis in the rat. *J Histochem Cytochem* 43: 895–905, 1995.
6. **Beyth S, Borovsky Z, Mevorach D, Liebergall M, Gazit Z, Aslan H, Galun E, Rachmilewitz J.** Human mesenchymal stem cells alter antigen-presenting cell maturation and induce T-cell unresponsiveness. *Blood* 105: 2214–2219, 2005.
7. **Border WA, Ruoslahti E.** Transforming growth factor-beta 1 induces extracellular matrix formation in glomerulonephritis. *Cell Differ Dev* 32: 425–431, 1990.
8. **Bussolati B, Tetta C, Camussi G.** Contribution of stem cells to kidney repair. *Am J Nephrol* 28: 813–822, 2008.
9. **Caterson EJ, Nesti LJ, Danielson KG, Tuan RS.** Human marrow-derived mesenchymal progenitor cells: isolation, culture expansion, and analysis of differentiation. *Mol Biotechnol* 20: 245–256, 2002.
10. **Cattell V.** Macrophages in acute glomerular inflammation. *Kidney Int* 45: 945–952, 1994.
11. **Chamberlain G, Fox J, Ashton B, Middleton J.** Concise review: mesenchymal stem cells: their phenotype, differentiation capacity, immunological features, and potential for homing. *Stem Cells* 25: 2739–2749, 2007.
12. **Corcione A, Benvenuto F, Ferretti E, Giunti D, Cappiello V, Cazzanti F, Risso M, Gualandi F, Mancardi GL, Pistoia V, Uccelli A.** Human mesenchymal stem cells modulate B-cell functions. *Blood* 107: 367–372, 2006.
13. **Di Nicola M, Carlo-Stella C, Magni M, Milanesi M, Longoni PD, Matteucci P, Grisanti S, Gianni AM.** Human bone marrow stromal cells suppress T-lymphocyte proliferation induced by cellular or nonspecific mitogenic stimuli. *Blood* 99: 3838–3843, 2002.
14. **Glennie S, Soeiro I, Dyson PJ, Lam EW, Dazzi F.** Bone marrow mesenchymal stem cells induce division arrest anergy of activated T cells. *Blood* 105: 2821–2827, 2005.
15. **Gonzalez-Rey E, Anderson P, Gonzalez MA, Rico L, Buscher D, Delgado M.** Human adult stem cells derived from adipose tissue protect against experimental colitis and sepsis. *Gut* 58: 929–939, 2009.
16. **Grimm PC, Nickerson P, Jeffery J, Savani RC, Gough J, McKenna RM, Stern E, Rush DN.** Neointimal and tubulointerstitial infiltration by recipient mesenchymal cells in chronic renal-allograft rejection. *N Engl J Med* 345: 93–97, 2001.
17. **Herrera MB, Bussolati B, Bruno S, Fonsato V, Romanazzi GM, Camussi G.** Mesenchymal stem cells contribute to the renal repair of acute tubular epithelial injury. *Int J Mol Med* 14: 1035–1041, 2004.
18. **In't Anker PS, Scherjon SA, Kleijburg-van der Keur C, de Groot-Swings GM, Claas FH, Fibbe WE, Kanhai HH.** Isolation of mesenchymal stem cells of fetal or maternal origin from human placenta. *Stem Cells* 22: 1338–1345, 2004.
19. **Isaka Y, Brees DK, Ikegaya K, Kaneda Y, Imai E, Noble NA, Border WA.** Gene therapy by skeletal muscle expression of decorin prevents fibrotic disease in rat kidney. *Nat Med* 2: 418–423, 1996.
20. **Ishikane S, Ohnishi S, Yamahara K, Sada M, Harada K, Mishima K, Iwasaki K, Fujiwara M, Kitamura S, Nagaya N, Ikeda T.** Allogeneic injection of fetal membrane-derived mesenchymal stem cells induces therapeutic angiogenesis in a rat model of hind limb ischemia. *Stem Cells* 26: 2625–2633, 2008.
21. **Ito T, Suzuki A, Imai E, Okabe M, Hori M.** Bone marrow is a reservoir of repopulating mesangial cells during glomerular remodeling. *J Am Soc Nephrol* 12: 2625–2635, 2001.
22. **Jones S, Horwood N, Cope A, Dazzi F.** The antiproliferative effect of mesenchymal stem cells is a fundamental property shared by all stromal cells. *J Immunol* 179: 2824–2831, 2007.
23. **Kale S, Karihaloo A, Clark PR, Kashgarian M, Krause DS, Cantley LG.** Bone marrow stem cells contribute to repair of the ischemically injured renal tubule. *J Clin Invest* 112: 42–49, 2003.
24. **Kawachi H, Oite T, Shimizu F.** Quantitative study of mesangial injury with proteinuria induced by monoclonal antibody 1-22-3. *Clin Exp Immunol* 92: 342–346, 1993.
25. **Kawachi H, Orikasa M, Matsui K, Iwanaga T, Toyabe S, Oite T, Shimizu F.** Epitope-specific induction of mesangial lesions with proteinuria by a MoAb against mesangial cell surface antigen. *Clin Exp Immunol* 88: 399–404, 1992.
26. **Kim J, Hematti P.** Mesenchymal stem cell-educated macrophages: a novel type of alternatively activated macrophages. *Exp Hematol* 37: 1445–1453, 2009.
27. **Krampera M, Cosmi L, Angeli R, Pasini A, Liotta F, Andreini A, Santarlasci V, Mazzinghi B, Pizzolo G, Vinante F, Romagnani P, Maggi E, Romagnani S, Annunziato F.** Role for interferon-gamma in the immunomodulatory activity of human bone marrow mesenchymal stem cells. *Stem Cells* 24: 386–398, 2006.
28. **Krampera M, Glennie S, Dyson J, Scott D, Laylor R, Simpson E, Dazzi F.** Bone marrow mesenchymal stem cells inhibit the response of naive and memory antigen-specific T cells to their cognate peptide. *Blood* 101: 3722–3729, 2003.
29. **Kreisberg JI, Karnovsky MJ.** Glomerular cells in culture. *Kidney Int* 23: 439–447, 1983.
30. **Kunter U, Rong S, Boor P, Eitner F, Muller-Newen G, Djuric Z, van Roeyen CR, Konieczny A, Ostendorf T, Villa L, Milovanceva-Popovska M, Kerjaschki D, Floege J.** Mesenchymal stem cells prevent progressive experimental renal failure but maldifferentiate into glomerular adipocytes. *J Am Soc Nephrol* 18: 1754–1764, 2007.
31. **Kunter U, Rong S, Djuric Z, Boor P, Muller-Newen G, Yu D, Floege J.** Transplanted mesenchymal stem cells accelerate glomerular healing in experimental glomerulonephritis. *J Am Soc Nephrol* 17: 2202–2212, 2006.
32. **Magnasco A, Corselli M, Bertelli R, Ibatici A, Peresi M, Gaggero G, Cappiello V, Chiavarina B, Mattioli G, Gusmano R, Ravetti JL, Frassoni F, Ghiggeri GM.** Mesenchymal stem cells protective effect in adriamycin model of nephropathy. *Cell Transplant* 17: 1157–1167, 2008.
33. **McTaggart SJ, Atkinson K.** Mesenchymal stem cells: immunobiology and therapeutic potential in kidney disease. *Nephrology* 12: 44–52, 2007.
34. **Mori T, Shimizu A, Masuda Y, Fukuda Y, Yamanaka N.** Hepatocyte growth factor-stimulating endothelial cell growth and accelerating glomerular capillary repair in experimental progressive glomerulonephritis. *Nephron* 94: e44–e54, 2003.
35. **Morigi M, Benigni A, Remuzzi G, Imberti B.** The regenerative potential of stem cells in acute renal failure. *Cell Transplant* 15, *Suppl* 1: S111–S117, 2006.
36. **Nagaya N, Kangawa K, Itoh T, Iwase T, Murakami S, Miyahara Y, Fujii T, Uematsu M, Ohgushi H, Yamagishi M, Tokudome T, Mori H, Miyatake K, Kitamura S.** Transplantation of mesenchymal stem cells improves cardiac function in a rat model of dilated cardiomyopathy. *Circulation* 112: 1128–1135, 2005.
37. **Nauta AJ, Kruisselbrink AB, Lurvink E, Willemze R, Fibbe WE.** Mesenchymal stem cells inhibit generation and function of both CD34+derived and monocyte-derived dendritic cells. *J Immunol* 177: 2080–2087, 2006.
38. **Nemeth K, Leelahavanichkul A, Yuen PS, Mayer B, Parmelee A, Doi K, Robey PG, Leelahavanichkul K, Koller BH, Brown JM, Hu X, Jelinek I, Star RA, Mezey E.** Bone marrow stromal cells attenuate sepsis via prostaglandin E_2-dependent reprogramming of host macrophages to increase their interleukin-10 production. *Nat Med* 15: 42–49, 2009.
39. **Ohnishi S, Sumiyoshi H, Kitamura S, Nagaya N.** Mesenchymal stem cells attenuate cardiac fibroblast proliferation and collagen synthesis through paracrine actions. *FEBS Lett* 581: 3961–3966, 2007.
40. **Ohnishi S, Yanagawa B, Tanaka K, Miyahara Y, Obata H, Kataoka M, Kodama M, Ishibashi-Ueda H, Kangawa K, Kitamura S, Nagaya N.** Transplantation of mesenchymal stem cells attenuates myocardial injury and dysfunction in a rat model of acute myocarditis. *J Mol Cell Cardiol* 42: 88–97, 2007.
41. **Ostendorf T, Kunter U, Eitner F, Loos A, Regele H, Kerjaschki D, Henninger DD, Janjic N, Floege J.** VEGF(165) mediates glomerular endothelial repair. *J Clin Invest* 104: 913–923, 1999.

42. **Pittenger MF, Mackay AM, Beck SC, Jaiswal RK, Douglas R, Mosca JD, Moorman MA, Simonetti DW, Craig S, Marshak DR.** Multilineage potential of adult human mesenchymal stem cells. *Science* 284: 143–147, 1999.
43. **Portmann-Lanz CB, Schoeberlein A, Huber A, Sager R, Malek A, Holzgreve W, Surbek DV.** Placental mesenchymal stem cells as potential autologous graft for pre- and perinatal neuroregeneration. *Am J Obstet Gynecol* 194: 664–673, 2006.
44. **Prodjosudjadi W, Gerritsma JS, van Es LA, Daha MR, Bruijn JA.** Monocyte chemoattractant protein-1 in normal and diseased human kidneys: an immunohistochemical analysis. *Clin Nephrol* 44: 148–155, 1995.
45. **Qian H, Yang H, Xu W, Yan Y, Chen Q, Zhu W, Cao H, Yin Q, Zhou H, Mao F, Chen Y.** Bone marrow mesenchymal stem cells ameliorate rat acute renal failure by differentiation into renal tubular epithelial-like cells. *Int J Mol Med* 22: 325–332, 2008.
46. **Rampino T, Gregorini M, Bedino G, Piotti G, Gabanti E, Ibatici A, Sessarego N, Piacenza C, Balenzano CT, Esposito P, Bosio F, Soccio G, Frassoni F, Dal Canton A..** Mesenchymal stromal cells improve renal injury in anti-Thy 1 nephritis by modulating inflammatory cytokines and scatter factors. *Clin Sci (Lond).* Epub ahead of print.
47. **Rookmaaker MB, Smits AM, Tolboom H, Van't Wout K, Martens AC, Goldschmeding R, Joles JA, Van Zonneveld AJ, Grone HJ, Rabelink TJ, Verhaar MC.** Bone-marrow-derived cells contribute to glomerular endothelial repair in experimental glomerulonephritis. *Am J Pathol* 163: 553–562, 2003.
48. **Rovin BH, Rumancik M, Tan L, Dickerson J.** Glomerular expression of monocyte chemoattractant protein-1 in experimental and human glomerulonephritis. *Lab Invest* 71: 536–542, 1994.
49. **Ryan JM, Barry FP, Murphy JM, Mahon BP.** Mesenchymal stem cells avoid allogeneic rejection. *J Inflamm (Lond)* 2: 8, 2005.
50. **Satriano JA, Hora K, Shan Z, Stanley ER, Mori T, Schlondorff D.** Regulation of monocyte chemoattractant protein-1 and macrophage colony-stimulating factor-1 by IFN-gamma, tumor necrosis factor-alpha, IgG aggregates, and cAMP in mouse mesangial cells. *J Immunol* 150: 1971–1978, 1993.
51. **Sotiropoulou PA, Perez SA, Gritzapis AD, Baxevanis CN, Papamichail M.** Interactions between human mesenchymal stem cells and natural killer cells. *Stem Cells* 24: 74–85, 2006.
52. **Spaggiari GM, Capobianco A, Abdelrazik H, Becchetti F, Mingari MC, Moretta L.** Mesenchymal stem cells inhibit natural killer-cell proliferation, cytotoxicity, and cytokine production: role of indoleamine 2,3-dioxygenase and prostaglandin E2. *Blood* 111: 1327–1333, 2008.
53. **Suga S, Kim YG, Joly A, Puchacz E, Kang DH, Jefferson JA, Abraham JA, Hughes J, Johnson RJ, Schreiner GF.** Vascular endothelial growth factor (VEGF121) protects rats from renal infarction in thrombotic microangiopathy. *Kidney Int* 60: 1297–1308, 2001.
54. **Sun L, Akiyama K, Zhang H, Yamaza T, Hou Y, Zhao S, Xu T, Le A, Shi S.** Mesenchymal stem cell transplantation reverses multiorgan dysfunction in systemic lupus erythematosus mice and humans. *Stem Cells* 27: 1421–1432, 2009.
55. **Tanaka T, Ichimaru N, Takahara S, Yazawa K, Hatori M, Suzuki K, Isaka Y, Moriyama T, Imai E, Azuma H, Nakamura T, Okuyama A, Yamanaka H.** In vivo gene transfer of hepatocyte growth factor to skeletal muscle prevents changes in rat kidneys after 5/6 nephrectomy. *Am J Transplant* 2: 828–836, 2002.
56. **Togel F, Cohen A, Zhang P, Yang Y, Hu Z, Westenfelder C.** Autologous and allogeneic marrow stromal cells are safe and effective for the treatment of acute kidney injury. *Stem Cells Dev* 18: 475–485, 2009.
57. **Uchida K, Nitta K, Kobayashi H, Kawachi H, Shimizu F, Yumura W, Nihei H.** Localization of Smad6 and Smad7 in the rat kidney and their regulated expression in the anti-Thy-1 nephritis. *Mol Cell Biol Res Commun* 4: 98–105, 2000.
58. **Uchimura H, Marumo T, Takase O, Kawachi H, Shimizu F, Hayashi M, Saruta T, Hishikawa K, Fujita T.** Intrarenal injection of bone marrow-derived angiogenic cells reduces endothelial injury and mesangial cell activation in experimental glomerulonephritis. *J Am Soc Nephrol* 16: 997–1004, 2005.
59. **Wang M, Yoshida A, Kawashima H, Ishizaki M, Takahashi H, Hori J.** Immunogenicity and antigenicity of allogeneic amniotic epithelial transplants grafted to the cornea, conjunctiva, and anterior chamber. *Invest Ophthalmol Vis Sci* 47: 1522–1532, 2006.
60. **Wenzel U, Schneider A, Valente AJ, Abboud HE, Thaiss F, Helmchen UM, Stahl RA.** Monocyte chemoattractant protein-1 mediates monocyte/macrophage influx in anti-thymocyte antibody-induced glomerulonephritis. *Kidney Int* 51: 770–776, 1997.
61. **Wong RK, Hagg EU, Rabie AB, Lau DW.** Bone induction in clinical orthodontics: a review. *Int J Adult Orthodon Orthognath Surg* 17: 140–149, 2002.
62. **Yokoo T, Kawamura T, Kobayashi E.** Stem cells for kidney repair: useful tool for acute renal failure? *Kidney Int* 74: 847–849, 2008.
63. **Zappia E, Casazza S, Pedemonte E, Benvenuto F, Bonanni I, Gerdoni E, Giunti D, Ceravolo A, Cazzanti F, Frassoni F, Mancardi G, Uccelli A.** Mesenchymal stem cells ameliorate experimental autoimmune encephalomyelitis inducing T-cell anergy. *Blood* 106: 1755–1761, 2005.

Regulatory Peptides 166 (2011) 21–27

Contents lists available at ScienceDirect

Regulatory Peptides

journal homepage: www.elsevier.com/locate/regpep

Adrenomedullin reduces expression of adhesion molecules on lymphatic endothelial cells

Donghao Jin [a], Kentaro Otani [a], Kenichi Yamahara [a,*], Tomoaki Ikeda [a], Noritoshi Nagaya [a], Kenji Kangawa [b]

[a] Department of Regenerative Medicine and Tissue Engineering, National Cardiovascular Center Research Institute, Osaka, Japan
[b] Department of Biochemistry, National Cardiovascular Center Research Institute, Osaka, Japan

ARTICLE INFO

Article history:
Received 15 March 2010
Received in revised form 26 July 2010
Accepted 11 August 2010
Available online 18 August 2010

Keywords:
Adrenomedullin
cAMP
Lymphatic endothelial cell
NF-kappaB
Microarray
Cell adhesion molecule

ABSTRACT

Adrenomedullin (AM) is a novel vasoactive peptide which regulates vascular tone and vascular endothelial cell growth. We recently reported that lymphatic endothelial cells (LECs) are also an attractive target of AM and concluded that AM is a potent mediator of lympangiogenesis. In the present study, we conducted a genome-wide analysis of genes that are regulated by AM in LECs. AM profoundly suppressed gene expression of cell adhesion receptors and inflammatory factors in LECs, such as intercellular adhesion molecule-1 (ICAM-1), vascular adhesion molecule-1 (VCAM-1), endothelial adhesion molecule-1 (E-selectin), interleukin-8, and chemokines, QRT-PCR and flow cytometry analysis showed that AM dose-dependently suppressed the TNF-a-induced mRNA and protein expression of ICAM-1 and VCAM-l. Treatment of LECs with a cell permeable cyclic adenosine monophosphate (cAMP) analog, 8-Br-cAMP, mimicked the suppressive effect of AM on the expression of adhesion molecules. Moreover, both AM and 8-Br-cAMP suppressed TNF-α-induced NF-κB activation in LECs, indicating that AM reduces expression of adhesion molecules in LECs via a cAMP/NF-kB dependent pathway. These results suggest that AM may have an important role in the regulation of the expression of adhesion molecules in lymphatic endothelium, which is critical in the control of immune and inflammatory responses.

1. Introduction

Adrenomedullin (AM) is a multifunctional peptide expressed and secreted from a variety of cells including vascular endothelial cells (ECs), vascular smooth muscle cells (SMCs), fibroblasts, and hematopoietic cells [1,2]. AM is known primarily for its' role in the vasculature and maintaining blood pressure [3,4], but recently AM has been implicated in the regulation of the inflammatory response [5–7]. In several inflammatory diseases, an elevated blood concentration of AM has been reported, and this increase has either a proinflammatory or an anti-inflammatory effect [8,9].

The lymphatic system is not only essential for maintenance of normal fluid balance, but also for proper immunologic function by providing an extensive network of vessels, needed for cell trafficking and immune responses. The interaction of lymphatic vessels and immunocytes has been well studied [10,11]. Lymphatic endothelium interacts with immunocytes through adhesion molecules and this interaction supports cell adhesion and migration [12]. Examples of two well known adhesion molecules involved in immunocyte adhesion and migration are: intercellular adhesion molecule-1 (ICAM1), which binds to lymphocyte function-associated antigen-1 (LFA-1) [13], and vascular cell adhesion molecule-1 (VCAM-1), which binds to the very late antigen 4 (α4β1) [14]. Increased expression of these adhesion molecules on lymphatic endothelium is found in the presence of inflammatory cytokines such as IL-1α or TNF-α [12]. Therefore, regulating the expression of these adhesion molecules in lymphatic endothelium is critical to control the immune and inflammatory responses.

Several studies have examined the role of AM or cyclic adenosine monophosphate (cAMP)-elevating agents in regulating the expression of adhesion molecules on vascular endothelium [15–18]. However, it is unknown whether AM or cAMP-elevating agents affect the expression of adhesion molecules on lymphatic endothelium. Recently, we reported that AM induces proliferation and migration of lymphatic endothelial cells (LECs) through a cAMP-dependent pathway [19] suggesting that AM may exert a critical role in the regulation of adhesive molecule expression on these cells through a cAMP-dependent pathway.

In this study, we investigated the effects of AM on gene expression in LECs by genome-wide analysis, and focused on the regulation of adhesion molecule expression by AM. We found that AM suppressed expression of genes involved in cell adhesion and inflammatory

* Corresponding author. Department of Regenerative Medicine and Tissue Engineering, National Cardiovascular Center Research Institute, 5-7-1 Fujishirodai, Suita, Osaka 565-8565, Japan. Tel.: +81 6 6833 5012; fax: +81 6 6835 5496.
E-mail address: yamahara@ri.ncvc.go.jp (K. Yamahara).

0167-0115/$ – see front matter © 2010 Elsevier B.V. All rights reserved.
doi:10.1016/j.regpep.2010.08.003

response; such as ICAM-1, VCAM-1, E-selectin, interleukin-8, TNF-α induced protein-2, -3, -8 and chemokine ligand-1, -2, -3, -20. We also found that AM significantly inhibited TNF-α-induced expression of ICAM-1, VCAM-1, E-selectin in LECs, and the inhibition was mediated by a cAMP/NF-κB dependent pathway.

2. Materials and methods

2.1. Cell culture

Human lymphatic microvascular endothelial cells (HLMVECs) were purchased from Lonza (Lonza, Basel, Switzerland), and expanded in basal medium (EBM-2, Lonza) with growth supplements (EGM-2MV, Lonza). All the cells were cultured on non-coating plastic dishes, and were used within passages 5–8. The expanded cells express mRNAs of the AM receptor calcitonin-receptor-like receptor (CRLR) and receptor-activity-modifying protein (RAMP)-1 to -3 [19].

2.2. Microarray

After 12 h of serum starvation in basal medium, HLMVECs were further cultured in EBM-2 supplemented with (10^{-7} M) or without AM (Sionogi, Osaka, Japan) for 4 hr. Total RNA was then isolated from the cells using an RNeasy mini kit (Qiagen, Hilden, Germany). Double-stranded cDNA was synthesized from total RNA, and in vitro transcription was performed to produce biotin-labeled cRNA using GeneChip One-Cycle Target Labeling and Control Reagents (Affymetrix, Santa Clara, CA, USA) according to the manufacturer's instructions. After fragmentation, the cRNA was hybridized with GeneChip (Affymetrix). GeneChips were then scanned in a GeneChip Scanner 3000 (Affymetrix). Normalization, filtering, and Gene Ontology analysis of the data were performed with GeneSpring GX 11 software (Agilent Technologies, Palo Alto, CA, USA). Genes with at least twofold change were then selected.

2.3. QRT-PCR

HLMVECs were grown in 6-cm plates and serum-starved for 12 hr in EBM-2. Cells were further incubated for 4 h in EBM-2 supplemented with 1) TNF-α (1 ng/ml, Peprotech, Rocky Hill, NJ, USA), 2) AM (10^{-7} M), 3) TNF-α and AM, 4) 3′, 5′-cyclic adenosine monophosphate 8-bromo sodium salt (8-Br-cAMP) 10^{-4} M, Calbiochem, San Diego, CA, USA , a cell-permeable cAMP analog, 5) TNF-α and 8-Br-cAMP. Total RNA was isolated from the cell lysate using RNeasy mini kit (Qiagen), and converted to cDNA by reverse transcription (QuantiTect RT-kit, Qiagen). QRT-PCR was performed with SYBR green dye (Qiagen) and a Prism 7700 sequence detection system (Applied Biosystems, Foster City, CA, USA). The PCR was carried out under the following conditions: an initial denaturation step at 95 °C for 10 min, followed by 40 cycles at 95 °C for 15 s and 60 °C for 60 s. Levels of ICAM-1, VCAM-1 and E-selectin mRNA were normalized to that of glyceraldehyde 3-phosphate dehydrogenase (GAPDH) mRNA. The PCR primers were summarized in Table 1 [20,21].

Table 1
Sequences of primers used in QRT-PCR.

	Forward	Reverse
ICAM-1	CGTGGGGAGAAGGAGCTGAA	CAGTGCGGCACGAGAAATTG
VCAM-1	TGGGCTGTGAATCCCCATCT	GGGTCAGCGCGTGGAATTGGTC
E-selectin	GATGAGAGGTGCAGCAAGAAG	CTCACACTTGAGTCCACTGAAG
GAPDH	TGAAGGTCGGTGTCAACGGATTTGGC	CATGTAGGCCATGAGGTCCACCAC

2.4. Flow cytometry

After 12 h of serum starvation in basal medium, HLMVECs were further cultured in EBM-2 supplemented with TNF-α (1 ng/ml), AM (10^{-7} M), or TNF-α and AM for 12 h. Cells were lifted by incubation for 10 min with collagenase (1 mg/ml, Wako, Osaka, Japan), and another 10 min with cell dissociation buffer (Invitrogen, Carlsbad, CA, USA), and collected in a cold PBS including 1% fetal bovine serum (FBS, Invitrogen). Collected cells were incubated for 30 min at 4 °C with FITC-conjugated anti-human ICAM-1 (CD54, Biolegend, San Diego, CA, USA) or PE-conjugated anti-human VCAM-1 (CD106, Biolegend), and analyzed on a flow cytometer (FACSCanto; BD, Franklin Lakes, NJ, USA). For the exclusion of nonviable cells, 7-AAD (BD) was added to each sample.

2.5. Preparation of subcellular protein fractions and Western blot analysis

Either cytoplasmic or nucleic proteins were extracted from cultured cells using CelLytic NuCLEAR Extraction Kit (Sigma, St. Louis, MO, USA) following the manufacturer's instruction. Briefly, cells were scarped and collected into centrifuge tubes using fresh PBS, and were then incubated in a hypotonic buffer including protease inhibitors, allowing cells to swell. The cells were then disrupted in a lysis buffer, and centrifuged at 10,000×*g*. The supernatant was transferred to a fresh tube as the cytoplasmic fraction. The crude pellet was resuspended in a nuclear extraction buffer and vortexed at high speed for 20 min. After centrifugation at 20,000×*g* for 5 min, the supernatant was transferred to a fresh tube as the nuclear fraction.

Cytoplasmic and nucleic proteins (2 μg) were denatured in SDS/DTT sampling buffer, loaded on 7.5% sodium dodecylsulfate-polyacrylamide gels (Bio-Rad, Hercules, CA, USA) for 90 min at 100 V, and transferred to membranes (Millipore, MA, USA) for 120 min at 100 V. After blocking with a solution of defatted milk, the membranes were probed with rabbit anti-NF-κB p65 polyclonal antibody (Santa Cruz Biotech, Santa Cruz, CA, USA). The membranes were then incubated with horseradish peroxidase-conjugated second antibodies (Cell Signaling, Boston, MA, USA), and visualized by ECL plus kit (GE Healthcare, Piscataway, NJ, USA) following the manufacturer's instruction.

2.6. Statistical analysis

All data are expressed as mean ± SEM. Comparisons of parameters among the groups were made by one-way ANOVA, followed by Newman-Keuls' test. Comparisons of parameters between two groups were made by Student's *t* test. Values of $p<0.05$ were considered statistically significant.

3. Results

3.1. Effect of AM on gene expression in LECs

We investigated the effect of AM on gene expression in LECs, using microarray analysis. After AM stimulation, 54 genes were upregulated (>twofold), and 150 genes were downregulated (<twofold) in HLMVECs (Tables 2 and 3). The cAMP related genes such as phosphodiesterase 4B, cAMP-specific, and cAMP responsive element modulators were upregulated after AM stimulation. In contrast, we found that genes involved in cell adhesion such as E-selectin, ICAM-1 and VCAM-1 and proinflammatory cytokines such as interleukin 8, TNF-α induced protein-2, -3, -8, and chemokine ligand-1, -2, -3, and -20 were downregulated after AM stimulation. In addition, expression of several NF-kB related elements such as nuclear factor of kappa light polypeptide gene enhancer in B-cells inhibitor, zeta (NFKBIZ), alpha

Table 2
Genes upregulated in HLMVEC after AM stimulation (>twofold).

Gene	Description	GenBank accession no.	Fold increase
PDK4	Pyruvate dehydrogenase kinase, isozyme 4	AV707102	5.954
PDK4	Pyruvate dehydrogenase kinase, isozyme 4	NM_002612	5.176
PDZRN3	PDZ domain containing RING finger 3	AL569804	3.319
EDNRB	Endothelin receptor type B	NM_000115	3.309
KIAA1126	Solute carrier family 45, member 4	AB032952	3.08
SEMA6A	Sema domain, transmembrane domain (TM), and cytoplasmic domain, (semaphorin) 6A	AB002438	2.938
	ye17h09.x5 Stratagene lung (#937210) *Homo sapiens* cDNA clone IMAGE:118049 3' similar to contains Alu repetitive element; mRNA sequence.	AI821404	2.921
SORBS1	Sorbin and SH3 domain containing 1	NM_015385	2.757
GAS1	Growth arrest-specific 1	NM_002048	2.74
PIK3R3	Phosphoinositide-3-kinase, regulatory subunit 3 (p55, gamma)	AF028785	2.656
	CDNA FLJ33091 fis, clone TRACH2000660	AK026379	2.629
HS3ST3B1	Heparan sulfate (glucosamine) 3-O-sulfotransferase 3B1	AA780067	2.549
CXCR4	Chemokine (C-X-C motif) receptor 4	AJ224869	2.548
TMEM100	Transmembrane protein 100	NM_018286	2.526
FRY	Furry homolog (Drosophila)	NM_023037	2.516
PDE4B	Phosphodiesterase 4B, cAMP-specific (phosphodiesterase E4 dunce homolog, Drosophila)	L20966	2.503
	CDNA FLJ26557 fis, clone LNF01992	AI970797	2.468
GPRIN3	GPRIN family member 3	AI819722	2.369
DKK1	dickkopf homolog 1 (*Xenopus laevis*)	NM_012242	2.368
PHF17	PHD finger protein 17	AV646599	2.359
TTC30B	Tetratricopeptide repeat domain 30B	BC033795	2.345
GOPC	Golgi associated PDZ and coiled-coil motif containing	AA279958	2.339
PDE4B	Phosphodiesterase 4B, cAMP-specific (phosphodiesterase E4 dunce homolog, Drosophila)	NM_002600	2.338
SFPQ	Splicing factor proline/glutamine-rich (polypyrimidine tract binding protein associated)	AI439021	2.326
HR	Hairless homolog (mouse)	BF528433	2.318
FREM3	FRAS1 related extracellular matrix 3	BE223071	2.305
MAB21L2	mab-21-like 2 (*C. elegans*)	AF262032	2.278
	yx52b04.s1 Soares melanocyte 2NbHM *Homo sapiens* cDNA clone IMAGE:265327 3', mRNA sequence.	N21096	2.261
TPR	Translocated promoter region (to activated MET oncogene)	AW235355	2.253
LOC387763	Hypothetical LOC387763	AW276078	2.251
ELMOD1	ELMO/CED-12 domain containing 1	AL359601	2.244
FAM84A	Family with sequence similarity 84, member A	AI601101	2.239
SLC45A4	Solute carrier family 45, member 4	AI346128	2.218
MN1	Meningioma (disrupted in balanced translocation) 1	NM_002430	2.209
FOLR1	Folate receptor 1 (adult)	AF000381	2.206
MIR	Myosin regulatory light chain interacting protein	NM_013262	2.203
C10orf72	Chromosome 10 open reading frame 72	BE858464	2.201
MYLIP	Myosin regulatory light chain interacting protein	T63512	2.195
CREM	cAMP responsive element modulator	D14826	2.193
NPTX1	Neuronal pentraxin I	NM_002522	2.184
PDGFRA	Platelet-derived growth factor receptor, alpha polypeptide	NM_006206	2.176
THSD1	Thrombospondin, type I, domain containing 1	NM_018676	2.165
RNF168	Ring finger protein 168	BC033791	2.156
MYLIP	Myosin regulatory light chain interacting protein	AW292746	2.15
SLCO2A1	Solute carrier organic anion transporter family, member 2A1	NM_005630	2.145
PROX1	Prospero homeobox 1	NM_002763	2.137
GOLSYN	Golgi-localized protein	NM_017786	2.116
PDXDC1	Pyridoxal-dependent decarboxylase domain containing 1	AI133523	2.115
SG2NA	Striatin, calmodulin binding protein 3	AF243424	2.113
ATRX	Alpha thalassemia/mental retardation syndrome X-linked (RAD54 homolog, *S. cerevisiae*)	AI650257	2.1
CDC42SE1	CDC42 small effector 1	AF286592	2.091
CREM	cAMP responsive element modulator	NM_001881	2.081
NASP	Nuclear autoantigenic sperm protein (histone-binding)	AU144734	2.064
ITPR1	Inositol 1,4,5-triphosphate receptor, type 1	U23850	2.047

(NFKBIA), and nuclear factor of kappa light polypeptide gene enhancer in B-cells inhibitor, epsilon (IKBE) were also decreased after treatment with AM.

3.2. Effect of AM on ICAM-1, VCAM-1 and E-selectin expression in LECs

QRT-PCR revealed that mRNA levels of ICAM-1, VCAM-1 and E-selectin were significantly reduced by AM treatment compared with the control (Fig. 1). Because the expression of ICAM-1, VCAM-1 and E-selectin in HLMVECs were significantly low. We treated the cells with TNF-α to increase expression of these adhesion molecules and TNF-α treatment led to a marked increase in the expression of these adhesive molecules [12]. In cultured HLMVECs, TNF-α treatment reduced CRLR expression (1.02 ± 0.10 vs. 0.68 ± 0.04, $p<0.05$) but did not alter RAMP-2 expression (1.09 ± 0.19 vs. 1.07 ± 0.12). TNF-α treatment in HLMVECs led to a marked increase of ICAM-1, VCAM-1 and E-selectin expression (ICAM-1; 1.14 ± 0.27 vs. 12.35 ± 2.78, VCAM-1; 1.06 ± 0.17 vs. 22.21 ± 5.39, E-selectin; 1.22 ± 0.35 vs. 19.85 ± 3.79, $p<0.01$), and this increase was significantly inhibited by 10^{-7} AM administration (ICAM-1; 5.13 ± 0.33, VCAM-1; 4.96 ± 0.84, E-selectin; 4.98 ± 0.94). AM dose-dependently inhibited the expression of these adhesion molecules in the range of 10^{-9}–10^{-7} M. Treatment of HLMVECs with a cell-permeable cAMP analog, 8-Br-cAMP (10^{-4} M), also significantly inhibited TNF-α-induced ICAM-1, VCAM-1 and E-selectin mRNA expression in HLMVECs (Fig. 1) (ICAM-1; 6.20 ± 0.60, VCAM-1; 5.35 ± 0.48, E-selectin; 8.41 ± 1.73, $p<0.01$). Next, we examined the protein levels of ICAM-1 and VCAM-1 in cultured HLMVECs (Fig. 2A and B). FACS analysis revealed that serum starved HLMVECs expressed low levels of ICAM-1 and VCAM-1. However, TNF-α treatment led to an approximately ten-fold increase in the expression of these adhesion molecules, but this effect was significantly dampened by AM administration (ICAM-1: 10.1 ± 0.2 vs. 7.2 ± 0.2, p-0.02; VCAM-1: 9.4 ± 0.2 vs. 6.7 ± 0.2, $p=0.01$). These results suggest that AM, and its second messenger cAMP inhibit the cell surface expression of the adhesion molecules ICAM-1 and VCAM-1, on LECs.

3.3. Effect of AM on NF-κB activation in LECs

In vascular ECs, TNF-α-induced expression of adhesion molecules is reported to be mediated through the activation of NF-κB [22]. Therefore, we examined whether TNF-α-induced NF-κB activation was inhibited by either AM or 8-Br-cAMP in HLMVECs. In resting cells, NF-kB lies within the cytoplasm in an inactive form. After NF-kB activation, the cytoplasmic NF-kB is activated and translocates to the nucleus [23]. Therefore, we measured the amount of NF-kB in the cytoplasm and the nucleus after AM stimulation (Fig. 3). Western blot analysis revealed that the nuclear concentration of NF-κB (105 KD and 65KD) was markedly increased in TNF-α-stimulated cells (2.2 ± 0.4-fold and 2.2 ± 0.2-fold vs. control, respectively) ($P<0.01$ vs. control), but this increase was inhibited by AM (0.4 ± 0.1-fold and 0.7 ± 0.1-fold vs.control, respectively) or 8-Br-cAMP treatment (0.2 ± 0.1-fold and 0.7 ± 0.2-fold vs control, respectively). These results suggest that

Table 3
Genes downregulated in HLMVEC after AM stimulation (<twofold).

Gene	Description	GenBank accession no.	Fold increase
SELE	Selectin E (endothelial adhesion molecule 1)	NM_000450	0.0813
CX3CL1	Chemokine (C-X3-C motif) ligand 1	U84487	0.0991
VCAM1	Vascular cell adhesion molecule 1	NM_001078	0.102
CCL20	Chemokine (C-C motif) ligand 20	NM_004591	0.119
F3	Coagulation factor III (thromboplastin, tissue factor)	NM_001993	0.126
ATF3	Activating transcription factor 3	NM_001674	0.127
BIC	BIC transcript	BG231961	0.169
SERPINE1	Serpin peptidase inhibitor, clade E (nexin, plasminogen activator inhibitor type 1), member 1	BC020765	0.172
IL8	*Homo sapiens* interleukin 8 C-terminal variant (IL8) mRNA, complete cds.	AF043337	0.181
NUAK2	NUAK family, SNF1-like kinase, 2	NM_030952	0.181
TRAF1	TNF receptor-associated factor 1	NM_005658	0.182
TRAF1	TNF receptor-associated factor 1	AA922208	0.201
TNFAIP8	Tumor necrosis factor, alpha-induced protein 8	NM_014350	0.23
CCL2	Chemokine (C-C motif) ligand 2	S69738	0.237
TNFAIP3	Tumor necrosis factor, alpha-induced protein 3	AI738896	0.239
TNFAIP3	Tumor necrosis factor, alpha-induced protein 3	NM_006290	0.243
HDAC9	Histone deacetylase 9	NM_014707	0.244
CX3CL1	Chemokine (C-X3-C motif) ligand 1	NM_002996	0.247
TMEM46	Transmembrane protein 46	AW664964	0.26
TNFAIP8	Tumor necrosis factor, alpha-induced protein 8	BC005352	0.262
EGR1	Early growth response 1	AI459194	0.265
BCL3	B-cell CLL/lymphoma 3	NM_005178	0.269
	CDNA clone IMAGE:5270500	BE467566	0.272
CXCL1	Chemokine (C-X-C motif) ligand 1 (melanoma growth stimulating activity, alpha)	NM_001511	0.272
ACY1L2	Aminoacylase 1-like 2	AI654133	0.273
	CDNA: FLJ23261 fis, clone COL05862	AK026914	0.274
BIRC3	Baculoviral IAP repeat-containing 3	U37546	0.281
FBXO32	F-box protein 32	AW006123	0.283
IL8	Interleukin 8	NM_000584	0.284
	Full length insert cDNA clone YX74D05	AI655467	0.286
CXCL2	Chemokine (C-X-C motif) ligand 2	M57731	0.289
ZC3H12C	Zinc finger CCCH-type containing 12C	AB051513	0.291
EGR3	early growth response 3	NM_004430	0.294
IRF1	Interferon regulatory factor 1	NM_002198	0.297
MAP3K8	Mitogen-activated protein kinase kinase kinase 8	NM_005204	0.3
	CDNA FLJ39585 fis, clone SKMUS2006633	N21643	0.305
CSF1	Colony stimulating factor 1 (macrophage)	M37435	0.309
LTB	Lymphotoxin beta (TNF superfamily, member 3)	NM_002341	0.312
	ag54e12.x5 Gessler Wilms tumor *Homo sapiens* cDNA clone IMAGE:1126798 3' similar to contains element MER36 repetitive element ;, mRNA sequence.	AI821759	0.315
CDKN2B	Cyclin-dependent kinase inhibitor 2B (p15, inhibits CDK4)	AW444761	0.315
CXCR7	Chemokine (C-X-C motif) receptor 7	AI817041	0.325
GBP1	Guanylate binding protein 1, interferon-inducible, 67 kDa	NM_002053	0.327
DUSP5	Dual specificity phosphatase 5	U16996	0.327
	AL536553 Homo sapiens FETAL BRAIN *Homo sapiens* cDNA clone CS0DF038YD07 3-PRIME, mRNA sequence.	AL536553	0.328
NFKBIZ	Nuclear factor of kappa light polypeptide gene enhancer in B-cells inhibitor, zeta	AB037925	0.329
EGR1	Early growth response 1	NM_001964	0.33
JUNB	Jun B proto-oncogene	NM_002229	0.331
BMP2	Bone morphogenetic protein 2	AA583044	0.335
RELB	v-rel reticuloendotheliosis viral oncogene homolog B, nuclear factor of kappa light polypeptide gene enhancer in B-cells 3 (avian)	NM_006509	0.341
SOD2	Superoxide dismutase 2, mitochondrial	AL050388	0.341
ZFP36	Zinc finger protein 36, C3H type, homolog (mouse)	NM_003407	0.346
TRIB1	Tribbles homolog 1 (Drosophila)	NM_025195	0.347
NLF1	Nuclear localized factor 1	BE218239	0.35
	MRNA; cDNA DKFZp547O0210 (from clone DKFZp547O0210)	AL831884	0.351
ZFP36L2	Zinc finger protein 36, C3H type-like 2	U07802	0.357
CAMTA1	Calmodulin binding transcription activator 1	AF111804	0.362
TNFAIP2	Tumor necrosis factor, alpha-induced protein 2	NM_006291	0.363
CAMTA1	Calmodulin binding transcription activator 1	Z98884	0.367
ZFP36L2	Zinc finger protein 36, C3H type-like 2	AI356398	0.367
NLF2	Nuclear localized factor 2	AI346522	0.371
MRCL3	Myosin regulatory light chain MRCL3	BU676221	0.371
NEDD4L	Neural precursor cell expressed, developmentally down-regulated 4-like	AV700008	0.371
BMP2A	Bone morphogenetic protein 2	NM_001200	0.374
SPRY4	Sprouty homolog 4 (Drosophila)	W48843	0.374
	Non-steroidal anti-inflammatory drug activated gene 3 mRNA, partial sequence	BE048571	0.374
RIPK2	Receptor-interacting serine-threonine kinase 2	AF064824	0.375
HECW2	HECT, C2 and WW domain containing E3 ubiquitin protein ligase 2	AL390186	0.376
LOC285628	Hypothetical protein LOC285628	AL389942	0.381
CXCL3	Chemokine (C-X-C motif) ligand 3	NM_002090	0.383
PTPRF	Protein tyrosine phosphatase, receptor type, F	AU158443	0.383
NEDD4L	Neural precursor cell expressed, developmentally down-regulated 4-like	AB007899	0.384
	CDNA: FLJ20903 fis, clone ADSE00222	AK024556	0.385
	601862985F1 NIH_MGC_57 *Homo sapiens* cDNA clone IMAGE:4080500 5', mRNA sequence.	BF244402	0.388
ATP8B1	ATPase, Class I, type 8B, member 1	BG290908	0.389
TRAK1	Trafficking protein, kinesin binding 1	AI633774	0.39
	UI-H-FH1-bfj-p-02-0-UI.s1 NCI_CGAP_FH1 *Homo sapiens* cDNA clone UI-H-FH1-bfj-p-02-0-UI 3', mRNA sequence.	BU617052	0.392
TAGLN	Transgelin	NM_003186	0.394
RIPK2	Receptor-interacting serine-threonine kinase 2	AF027706	0.395
	CDNA FLJ12055 fis, clone HEMBB1002049	AU146983	0.402
PLA2G4C	Phospholipase A2, group IVC (cytosolic, calcium-independent)	BC017956	0.405
SOX7	SRY (sex determining region Y)-box 7	BC004299	0.407
GLIS2	GLIS family zinc finger 2	AA705182	0.41
	MRNA; cDNA DKFZp586G1917 (from clone DKFZp586G1917)	AL117453	0.41
GBP1	Guanylate binding protein 1, interferon-inducible, 67 kDa	BC002666	0.412
VEGFC	Vascular endothelial growth factor C	U58111	0.413
TRAK1	trafficking protein, kinesin binding 1	AK000754	0.416
GBP1	Guanylate binding protein 1, interferon-inducible, 67 kDa	AW014593	0.417
KCNN2	Potassium intermediate/small conductance calcium-activated channel, subfamily N, member 2	NM_021614	0.417
C13orf31	Chromosome 13 open reading frame 31	NM_153218	0.424
TRIB1	Tribbles homolog 1 (Drosophila)	AA576947	0.424
RGS7	Regulator of G-protein signalling 7	NM_002924	0.425
IFIH1	Interferon induced with helicase C domain 1	BC046208	0.426
NFKBIZ	Nuclear factor of kappa light polypeptide gene enhancer in B-cells inhibitor, zeta	BE646573	0.426
ICAM1	Intercellular adhesion molecule 1 (CD54), human rhinovirus receptor	NM_000201	0.428
IER2	Immediate early response 2	NM_004907	0.43
	601659282R1 NIH_MGC_70 *Homo sapiens* cDNA clone IMAGE:3895653 3', mRNA sequence.	BE965369	0.431
GSTM4	Glutathione S-transferase M4	NM_000850	0.431
RND1	Rho family GTPase 1	U69563	0.432
ZFP36L2	Zinc finger protein 36, C3H type-like 2	NM_006887	0.434
TRAK1	Trafficking protein, kinesin binding 1	NM_014965	0.437
NUMB	Numb homolog (Drosophila)	AW167424	0.438

Table 3 *(continued)*

Gene	Description	GenBank accession no.	Fold increase
KLF10	Kruppel-like factor 10	NM_005655	0.44
BHLHE40	Basic helix-loop-helix domain containing, class B, 2	NM_003670	0.441
IKBE	Nuclear factor of kappa light polypeptide gene enhancer in B-cells inhibitor, epsilon	NM_004556	0.442
MGC16121	Hypothetical protein MGC16121	AA234096	0.443
	DNF1552 protein; Human DNF1552 (lung) mRNA, complete cds.	J03068	0.444
	601862985F1 NIH_MGC_57 *Homo sapiens* cDNA clone IMAGE:4080500 5', mRNA sequence.	BF244402	0.444
CYLD	Cylindromatosis (turban tumor syndrome)	BE046443	0.448
GUCY1B3	Guanylate cyclase 1, soluble, beta 3	W93728	0.45
CYLD	Cylindromatosis (turban tumor syndrome)	AA555096	0.45
B4GALT1	UDP-Gal:betaGlcNAc beta 1,4-galactosyltransferase, polypeptide 1	AL574435	0.452
PLEKHG1	Pleckstrin homology domain containing, family G (with RhoGef domain) member 1	AL035086	0.452
NMT2	N-myristoyltransferase 2	AK025065	0.453
CYLD	Cylindromatosis (turban tumor syndrome)	AK024212	0.454
USP54	Ubiquitin specific peptidase 54	AW242125	0.454
SOX7	SRY (sex determining region Y)-box 7	AI808807	0.454
SAMD4A	Sterile alpha motif domain containing 4A	AB028976	0.455
	ht13b05.x1 NCI_CGAP_Kid13 *Homo sapiens* cDNA clone IMAGE:3146577 3' similar to contains MER28.b2 MER28 repetitive element; mRNA sequence.	BE350312	0.456
IFIH1	Interferon induced with helicase C domain 1	NM_022168	0.457
NEDD4L	Neural precursor cell expressed, developmentally down-regulated 4-like	AI357376	0.458
	CDNA FLJ33153 fis, clone UTERU2000332	AW467415	0.458
ARL4C	ADP-ribosylation factor-like 4C	BG435404	0.459
DUSP8	Dual specificity phosphatase 8	NM_004420	0.462
PLAU	Plasminogen activator, urokinase	K03226	0.462
LOC401317	Hypothetical LOC401317	AW071804	0.464
CCRN4L	CCR4 carbon catabolite repression 4-like (*S. cerevisiae*)	BC021963	0.465
	CDNA FLJ11570 fis, clone HEMBA1003309	AU157224	0.468
EGR2	Early growth response 2 (Krox-20 homolog, Drosophila)	NM_000399	0.471
NFKBIA	Nuclear factor of kappa light polypeptide gene enhancer in B-cells inhibitor, alpha	AI078167	0.471
PDE5A	Phosphodiesterase 5A, cGMP-specific	BF221547	0.473
UBD	Ubiquitin D	NM_006398	0.474
EDG3	Endothelial differentiation, sphingolipid G-protein-coupled receptor, 3	AA534817	0.476
ATF3	Activating transcription factor 3	AB066566	0.478
c-fos	v-fos FBJ murine osteosarcoma viral oncogene homolog	BC004490	0.479
BACH2	BTB and CNC homology 1, basic leucine zipper transcription factor 2	NM_021813	0.479
BCL3	B-cell CLL/lymphoma 3	AI829875	0.479
GUCY1A3	Guanylate cyclase 1, soluble, alpha 3	AI719730	0.48
COBLL1	COBL-like 1	BF002844	0.483
ARHGEF10	Rho guanine nucleotide exchange factor (GEF) 10	BC040474	0.484
LMCD1	LIM and cysteine-rich domains 1	N95437	0.486
F2RL1	Coagulation factor II (thrombin) receptor-like 1	NM_005242	0.488
KLF9	Kruppel-like factor 9	NM_001206	0.488
TBX3	T-box 3 (ulnar mammary syndrome)	NM_016569	0.489
EFNA1	Ephrin-A1	NM_004428	0.489
CITED4	Cbp/p300-interacting transactivator, with Glu/Asp-rich carboxy-terminal domain, 4	AI858001	0.49
HBEGF	Heparin-binding EGF-like growth factor	NM_001945	0.492
CYLD	Cylindromatosis (turban tumor syndrome)	AL050166	0.492
CALD1	Caldesmon 1	AU147402	0.493
CMTM7	CKLF-like MARVEL transmembrane domain containing 7	AL832450	0.494
ITGA4	Integrin, alpha 4 (antigen CD49D, alpha 4 subunit of VLA-4 receptor)	BG532690	0.495

AM and its second messenger cAMP, inhibit the activation of NF-κB in LECs.

4. Discussion

We have recently reported that AM strongly induces elevation of intracellular cAMP in LECs and promotes cell proliferation [19]. In this study, we investigated the effect of AM on gene expression in LECs, and focused on the adhesion molecules whose expression is shown to be regulated by AM. Our results showed that 1) AM suppressed expression of genes involved in cell adhesion and inflammatory responses, such as E-selectin, ICAM-1, VCAM-1, interleukin-8, TNF-α induced protein-2, -3, and -8 and chemokine ligand-1, -2, -3, and -20. 2) AM inhibited TNF-α-induced ICAM-1, VCAM-1 expression in LECs, and this inhibition was mediated by the elevation of cellular cAMP and down-regulation of its downstream effector NF-κB.

During the onset of tissue inflammatory response, the concentration of AM is increased. Examples of this include the increase in plasma AM after endotoxin administration, and in inflammatory diseases like sepsis and systemic inflammatory response syndrome [24–26]. The relationship between AM and the proinflammatory cytokine network is complicated; proinflammatory factors including TNF-α, lipopolysaccharide (LPS), and IL-1 increase AM production in ECs, SMCs, and macrophages/monocytes, and AM suppresses IL-1β-induced TNF-α production in Swiss 3T3 cells [27–30]. In addition, AM downregulates proinflammatory cytokine production in sepsis [28,31]. In our microarray analysis, AM suppressed the expression of genes involved in inflammatory responses, such as interleukin-8, TNF-α induced protein-2, -3, and -8 and chemokine ligand-1, -2, -3, and -20 in LECs. Therefore, we speculate that many cells within the inflammatory system including vascular and lymphatic ECs/SMCs and macrophages/monocytes seem to secrete AM, its production would be stimulated by inflammatory factors, and secreted AM appears to downregulate the production of inflammatory cytokines in the inflammatory system, which may result in less tissue inflammation.

In blood vascular endothelium, the effect of AM on adhesion molecules expression has been investigated previously, but the findings are conflicting. In human umbilical vein ECs (HUVECs), AM has been reported to induce ICAM-1 and VCAM-1 expression by elevation of cAMP [15]. Although we examined the effect of AM in HUVECs, AM itself did not change the expression of these adhesion molecules (data not shown). Kim et al. reported that AM reduced VEGF-induced ICAM-1 and VCAM-1 expression in HUVECs [16]. Other studies of the role of cAMP on adhesion molecule expression in HUVECs found that cAMP down-regulated TNF-α-stimulated endothelial ICAM-1 or VCAM-1 expression through down-regulation of transcription factor NF-κB [17,18]. In the present study, we found that AM itself markedly reduced the gene expression of a series of TNF-α-induced proteins in HLMVECs, which did not observed in HUVECs (data not shown), and would indicate the suppressive effect of AM on TNF-α-induced cellular actions. QRT-PCR and FACS analysis revealed that AM significantly suppressed TNF-α-induced expression of ICAM-1, VCAM-1 and E-selectin in LECs. AM also suppressed TNF-α-induced translocation of NF-κB from the cytoplasm to the nucleus in LECs. This suggests that AM inhibits the expression of adhesion molecules in TNF-α-stimulated LECs, and that this inhibition is mediated by suppression of NF-κB activation.

In conclusion, our study demonstrates that AM suppresses adhesion molecules including ICAM-1, VCAM-1, E-selectin expression in LECs via the elevation of cellular cAMP and down-regulation of its downstream effector NF-κB. Thus, AM may play an important role in the inflammatory and immune response by regulating the expression of cell adhesion molecules on lymphatic endothelium.

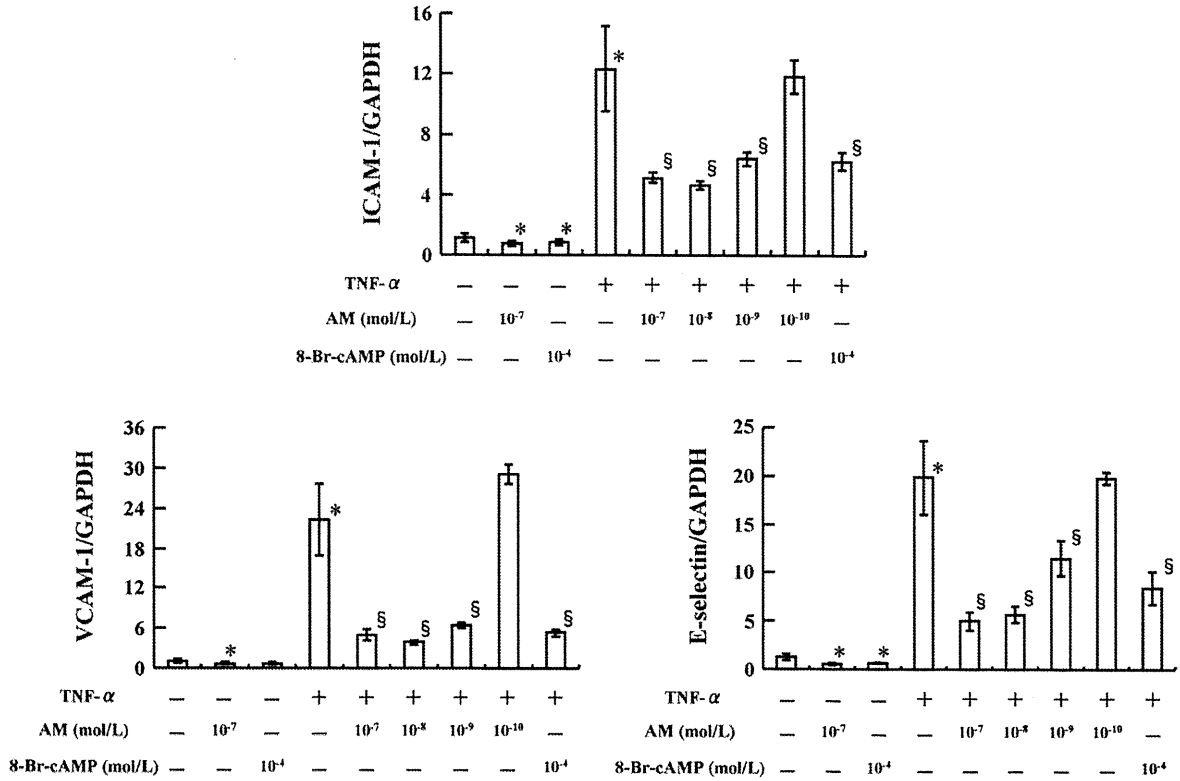

Fig. 1. AM and cAMP suppressed mRNA expression of ICAM-1, VCAM-1 and E-selectin in TNF-α-treated HLMVECs. Cells were cultured for 4 h with indicated agents, and mRNA levels were measured by QRT-PCR. Levels were normalized to that of GAPDH mRNA. Relative gene expression levels of ICAM-1 (A), VCAM-1 (B) and E-selectin (C) are shown after the treatment with AM, 8-Br-cAMP, TNF-α, TNF-α and AM or TNF-α and 8-Br-cAMP. Data are mean ± SEM. n = 5–10. *$p<0.05$ vs. non-treated cell. §$p<0.05$ vs. TNF-α stimulated cells.

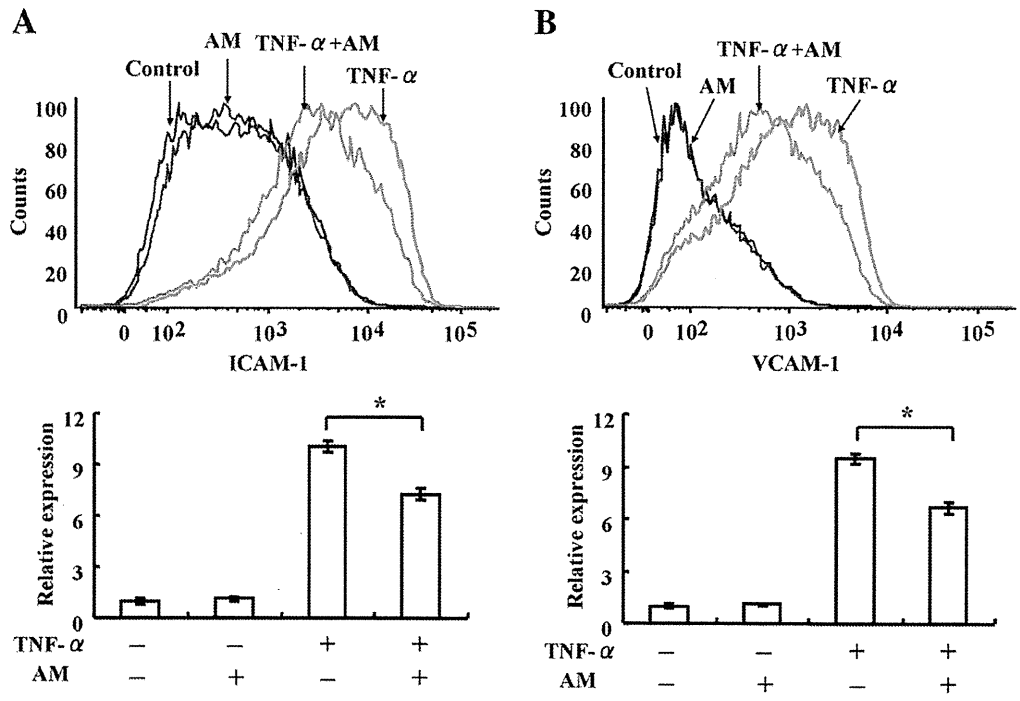

Fig. 2. AM suppressed cell surface expression of ICAM-1 and VCAM-1 on TNF-α-treated HLMVECs. Cells were cultured for 12 h in the absence (Control) or presence of AM, TNF-α or TNF-α and AM (TNF-α + AM). Upper panels show FACS histograms of HLMVECs after the staining with either ICAM-1 (A) or VCAM-1 (B). Lower panels show the mean fluorescence intensity of these adhesion molecules by FACS analysis. Data are mean ± SD. n = 3. *$p<0.05$.

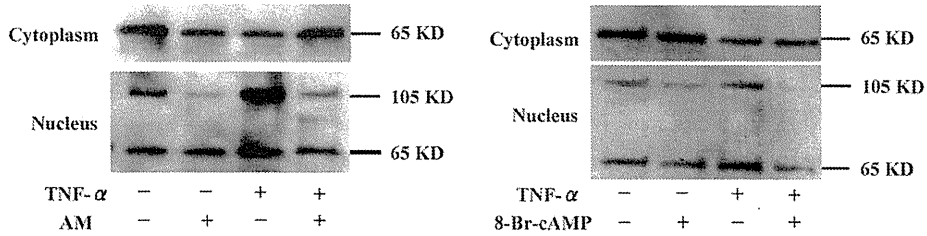

Fig. 3. AM and cAMP suppressed activation of NF-κB in TNF-α-treated HLMVECs. Cells were cultured for 1 h with the indicated agents, cytoplasmic and nucleic proteins were extracted, and the concentration of NF-κB was measured by Western blot analysis. (A) Representative blotting images of NF-κB are shown after the treatment with AM, TNF-α or TNF-α and AM. (B) Representative blotting images of NF-κB are shown after the treatment with 8-Br-cAMP, TNF-α or TNF-α and 8-Br-cAMP.

Acknowledgements

Funding for this work was provided by research grants for Cardiovascular Disease (19C-7) from the Ministry of Health, Labour and Welfare; the Program for Promotion of Fundamental Studies in Health Sciences of the National Institute of Biomedical Innovation (NIBIO); and the Japan Vascular Disease Research Foundation.

References

[1] Tomoda Y, Isumi Y, Katafuchi T, Minamino N. Regulation of adrenomedullin secretion from cultured cells. Peptides 2001;22:1783–94.
[2] Hinson JP, Kapas S, Smith DM. Adrenomedullin, a multifunctional regulatory peptide. Endocr Rev 2000;21:138–67.
[3] Kato J, Kitamura K, Eto T. Plasma adrenomedullin level and development of hypertension. J Hum Hypertens 2006;20:566–70.
[4] Shindo T, Kurihara Y, Nishimatsu H, Moriyama N, Kakoki M, Wang Y, Imai Y, Ebihara A, Kuwaki T, Ju KH, Minamino N, Kangawa K, Ishikawa T, Fukuda M, Akimoto Y, Kawakami H, Imai T, Morita H, Yazaki Y, Nagai R, et al. Vascular abnormalities and elevated blood pressure in mice lacking adrenomedullin gene. Circulation 2001;104:1964–71.
[5] Elsasser TH, Kahl S. Adrenomedullin has multiple roles in disease stress: development and remission of the inflammatory response. Microsc Res Tech 2002;57:120–9.
[6] Allaker RP, Zihni C, Kapas S. An investigation into the antimicrobial effects of adrenomedullin on members of the skin, oral, respiratory tract and gut microflora. FEMS Immunol Med Microbiol 1999;23:289–93.
[7] Martinez A, Elsasser TH, Muro-Cacho C, Moody TW, Miller MJ, Macri CJ, Cuttitta F. Expression of adrenomedullin and its receptor in normal and malignant human skin: a potential pluripotent role in the integument. Endocrinology 1997;138: 5597–604.
[8] Clementi G, Floriddia ML, Prato A, Marino A, Drago F. Adrenomedullin and ocular inflammation in the rabbit. Eur J Pharmacol 2000;400:321–6.
[9] Clementi G, Caruso A, Cutuli VM, Prato A, Mangano NG, Amico-Roxas M. Antiinflammatory activity of adrenomedullin in the acetic acid peritonitis in rats. Life Sci 1999;65:PL203–8.
[10] Randolph GJ, Angeli V, Swartz MA. Dendritic-cell trafficking to lymph nodes through lymphatic vessels. Nat Rev Immunol 2005;5:617–28.
[11] Angeli V, Randolph GJ. Inflammation, lymphatic function, and dendritic cell migration. Lymphat Res Biol 2006;4:217–28.
[12] Johnson LA, Clasper S, Holt AP, Lalor PF, Baban D, Jackson DG. An inflammation-induced mechanism for leukocyte transmigration across lymphatic vessel endothelium. J Exp Med 2006;203:2763–77.
[13] Makgoba MW, Sanders ME, Ginther Luce GE, Gugel EA, Dustin ML, Springer TA, Shaw S. Functional evidence that intercellular adhesion molecule-1 (ICAM-1) is a ligand for LFA-1-dependent adhesion in T cell-mediated cytotoxicity. Eur J Immunol 1988;18:637–40.
[14] Elices MJ, Osborn L, Takada Y, Crouse C, Luhowskyj S, Hemler ME, Lobb RR. VCAM-1 on activated endothelium interacts with the leukocyte integrin VLA-4 at a site distinct from the VLA-4/fibronectin binding site. Cell 1990;60:577–84.
[15] Hagi-Pavli E, Farthing PM, Kapas S. Stimulation of adhesion molecule expression in human endothelial cells (HUVEC) by adrenomedullin and corticotrophin. Am J Physiol Cell Physiol 2004;286:C239–46.
[16] Kim W, Moon SO, Lee S, Sung MJ, Kim SH, Park SK. Adrenomedullin reduces VEGF-induced endothelial adhesion molecules and adhesiveness through a phosphatidylinositol 3'-kinase pathway. Arterioscler Thromb Vasc Biol 2003;23:1377–83.
[17] Pober JS, Slowik MR, De Luca LG, Ritchie AJ. Elevated cyclic AMP inhibits endothelial cell synthesis and expression of TNF-induced endothelial leukocyte adhesion molecule-1, and vascular cell adhesion molecule-1, but not intercellular adhesion molecule-1. J Immunol 1993;150:5114–23.
[18] Parry GC, Mackman N. Role of cyclic AMP response element-binding protein in cyclic AMP inhibition of NF-kappaB-mediated transcription. J Immunol 1997;159: 5450–6.
[19] Jin D, Harada K, Ohnishi S, Yamahara K, Kangawa K, Nagaya N. Adrenomedullin induces lymphangiogenesis and ameliorates secondary lymphoedema. Cardiovasc Res 2008;80:339–45.
[20] Migita H, Satozawa N, Lin JH, Morser J, Kawai K. RORalpha1 and RORalpha4 suppress TNF-alpha-induced VCAM-1 and ICAM-1 expression in human endothelial cells. FEBS Lett 2004;557:269–74.
[21] Ohnishi S, Sumiyoshi H, Kitamura S, Nagaya N. Mesenchymal stem cells attenuate cardiac fibroblast proliferation and collagen synthesis through paracrine actions. FEBS Lett 2007;581:3961–6.
[22] Siebenlist U, Franzoso G, Brown K. Structure, regulation and function of NF-kappa B. Annu Rev Cell Biol 1994;10:405–55.
[23] Baldwin Jr AS. The NF-kappa B and I kappa B proteins: new discoveries and insights. Annu Rev Immunol 1996;14:649–83.
[24] Hattori Y, Murakami Y, Atsuta H, Minamino N, Kangawa K, Kasai K. Glucocorticoid regulation of adrenomedullin in a rat model of endotoxic shock. Life Sci 1998;62: PL181–9.
[25] Hirata Y, Mitaka C, Sato K, Nagura T, Tsunoda Y, Amaha K, Marumo F. Increased circulating adrenomedullin, a novel vasodilatory peptide, in sepsis. J Clin Endocrinol Metab 1996;81:1449–53.
[26] Ueda S, Nishio K, Minamino N, Kubo A, Akai Y, Kangawa K, Matsuo H, Fujimura Y, Yoshioka A, Masui K, Doi N, Murao Y, Miyamoto S. Increased plasma levels of adrenomedullin in patients with systemic inflammatory response syndrome. Am J Respir Crit Care Med 1999;160:132–6.
[27] Sugo S, Minamino N, Shoji H, Kangawa K, Kitamura K, Eto T, Matsuo H. Interleukin-1, tumor necrosis factor and lipopolysaccharide additively stimulate production of adrenomedullin in vascular smooth muscle cells. Biochem Biophys Res Commun 1995;207:25–32.
[28] Isumi Y, Minamino N, Kubo A, Nishimoto N, Yoshizaki K, Yoshioka M, Kangawa K, Matsuo H. Adrenomedullin stimulates interleukin-6 production in Swiss 3T3 cells. Biochem Biophys Res Commun 1998;244:325–31.
[29] Nakayama M, Takahashi K, Murakami O, Murakami H, Sasano H, Shirato K, Shibahara S. Adrenomedullin in monocytes and macrophages: possible involvement of macrophage-derived adrenomedullin in atherogenesis. Clin Sci (Lond) 1999;97:247–51.
[30] Kubo A, Minamino N, Isumi Y, Katafuchi T, Kangawa K, Dohi K, Matsuo H. Production of adrenomedullin in macrophage cell line and peritoneal macrophage. J Biol Chem 1998;273:16730–8.
[31] Koo DJ, Yoo P, Cioffi WG, Bland KI, Chaudry IH, Wang P. Mechanism of the beneficial effects of pentoxifylline during sepsis: maintenance of adrenomedullin responsiveness and downregulation of proinflammatory cytokines. J Surg Res 2000;91:70–6.

ELSEVIER

The Journal of
Heart and Lung
Transplantation
http://www.jhltonline.org

Quantitative assessment of initial retention of bone marrow mononuclear cells injected into the coronary arteries

Satsuki Fukushima, MD, PhD,[a] Niall G. Campbell, MRCP,[b] Steven R. Coppen, PhD,[b] Kenichi Yamahara, MD, PhD,[a] Ada H.Y. Yuen, BSc,[a] Ryzard T. Smolenski, MD, PhD,[a,c] Magdi H. Yacoub, FRS,[a] and Ken Suzuki, MD, PhD[a,b]

[a]*From the Harefield Heart Science Centre, Imperial College London, London, UK;*
[b]*William Harvey Research Institute, Barts and the London School of Medicine and Dentistry, Queen Mary, University of London, London, UK; and* [c]*Department of Biochemistry, Medical University of Gdansk, Gdansk, Poland.*

KEYWORDS:
cell transplantation;
heart;
bone marrow–derived stem cell;
cell adhesion molecules;
ischemia–reperfusion

BACKGROUND: Intracoronary injection of bone marrow mononuclear cells (BMMNC) is a common clinical protocol of cell transplantation for heart disease, but poor engraftment of donor cells in the heart, which will limit its therapeutic efficacy, is a major issue. Initial "retention" (endothelial adherence and/or extravasation) of BMMNC immediately after intracoronary injection is a key step toward successful engraftment; however, this event has not been fully characterized. The aim of this study is to quantitatively clarify the frequency of "retention" of BMMNC after intracoronary injection, determine the impact of prior induction of ischemia–reperfusion injury on "retention" efficiency, and elucidate the underlying mechanisms focusing on adhesion molecule–mediated cell–cell interactions.
METHODS: One million BMMNC collected from green fluorescent protein (GFP)-transgenic mice were injected into the coronary arteries of syngeneic wild-type mouse hearts under Langendorff perfusion. Retention efficiency was quantitatively estimated from the GFP-positive cell number flushed out into the coronary effluent.
RESULTS: Whereas only 13.3 ± 1.2% of injected BMMNC were retained into normal hearts, prior induction of 30-minute ischemia and 30-minute reperfusion increased the retention efficiency to 36.5 ± 1.6% ($p < 0.05$, $n = 8$). Immunoconfocal observation further confirmed this enhanced retention after ischemia–reperfusion. Noticeably, the enhanced retention efficiency after ischemia–reperfusion treatment was diminished by administration of anti–P-selectin antibody (8.3 ± 0.8%, $p < 0.05$), but was not affected by inhibiting intercellular adhesion molecule-1 (39.6 ± 3.3%) or vascular cell adhesion molecule-1 (43.9 ± 2.9%).
CONCLUSIONS: Retention efficiency of intracoronary-injected BMMNC was poor in a model of isolated, crystalloid-perfused murine hearts. An antecedent period of global ischemia–reperfusion increased the retention via P-selectin–dependent BMMNC–endothelial interaction.
J Heart Lung Transplant 2011;30:227–33

Although intracoronary injection of bone marrow mononuclear cells (BMMNC) is a promising treatment for heart disease,[1–3] further understanding and refinement are needed for future clinical success. It has been reported that only a few BMMNC persist and survive within the heart after intracoronary injection,[4–6] and this is likely to be a major limiting factor in therapeutic efficacy. Therefore, dissecting the factors responsible for poor engraftment of BMMNC will be valuable for developing new methods to improve the therapeutic efficacy of BMMNC transplantation. We consider that, in addition to donor cell death,[7] insufficient initial "retention" is a major cause of such poor engraftment of injected BMMNC. Herein we propose that initial "retention" of intracoronary-injected BMMNC includes: (i) passive and/or active adhesion to the endothelium; and (ii) subsequent extravasation (transendothelial migration) into the myocardial interstitium or integration into the vasculature. However, at present, the quantitative frequency of these cellular events after intracoronary injec-

Reprint requests: Ken Suzuki, MD, PhD, William Harvey Research Institute, Barts and the London School of Medicine, Charterhouse Square, London EC1M 6BQ, UK. Telephone: 44-20-7882-8233. Fax: 44-20-7882-8256.
E-mail address: ken.suzuki@qmul.ac.uk

1053-2498/$ -see front matter
doi:10.1016/j.healun.2010.09.002

tion and the molecular mechanisms responsible are not fully understood.

The initial retention of donor cells is likely to be mediated by adhesion molecules, similarly to the leukocyte–endothelial interaction. Ryzhov et al suggested the involvement of interaction between P-selectin and P-selectin glycoprotein ligand (PSGL)-1, the sole ligand of P-selectin, in adhesion between endothelial progenitor cells and endothelial cells, using an in vitro model.[8] It has also been shown that intercellular adhesion molecule (ICAM)-1 and vascular cell adhesion molecule (VCAM)-1 play a role in the retention of endothelial progenitor cells and mesenchymal stem cells, respectively.[9,10] However, in those earlier studies, the investigators used cells other than BMMNC and also did not administer cells into the coronary arteries, such as occurs in the clinical scenario. Furthermore, expression profiles of adhesion molecules of the coronary endothelium are known to be modulated by ischemia–reperfusion (I/R) injury,[11] giving the rise to the hypothesis that I/R induction prior to BMMNC injection alters retention efficiency. In this study, we quantitatively clarified the frequency of initial retention of BMMNC after intracoronary injection, determined the impact of the prior induction of I/R on the retention efficiency, and investigated the underlying mechanisms focusing on adhesion molecule–mediated cell–cell interactions.

Methods

All animal studies were carried out with the approval of the institutional ethics committee and the UK Home Office. Our investigation conformed to the Principles of Laboratory Animal Care formulated by the National Society for Medical Research and the *Guide for the Care and Use of Laboratory Animals* (U.S. National Institutes of Health Publication No. 85-23, revised 1996). All experimental procedures and evaluations were carried out in a blinded manner.

Collection and characterization of BMMNC

Bone marrow cells were collected from transgenic C57BL/6J mice expressing green fluorescent protein (GFP) under the human ubiquitin-C promoter (18 to 20 g; Jackson Laboratory).[12] BMMNC were then purified using Percoll gradient.[13] For characterization, BMMNC were labeled with monoclonal antibodies against PSGL-1 (BD Pharmingen), CD18 (eBioscience), Sca-1 (eBioscience), CD45 (eBioscience), CD34 (BD Pharmingen) and c-kit (eBioscience), followed by incubation with 7-amino actinomycin D (7-ADD; eBioscience). Samples were analyzed using FACSARIA and CELLQUEST software (BD Biosciences).[14]

Isolated heart perfusion

Hearts of wild-type C57BL/6J mice (Harlan) were perfused using a modified Langendorff apparatus with Krebs–Henseleit buffer at a constant pressure of 100 cm H_2O.[15]

Cell injection, ischemia–reperfusion and quantitative assessment of retention

Hearts under Langendorff perfusion were assigned to either the Normal group or I/R group after 20 minutes stabilization ($n = 8$ in each). For the Normal group, 1×10^6 BMMNC suspended in 1 ml of the buffer at 37°C were slowly injected from the side-port of the aortic cannula over 1 minute while the main perfusion was halted. Cell injection was a single, one-time infusion (no recirculation). For the I/R group, 30-minute global (whole coronary system) ischemia by zero perfusion and 30-minute reperfusion was induced after the stabilization, followed by BMMNC injection in the same manner.

Effluent of the Langendorff perfusion was continuously collected to measure the coronary flow every 1 minute from the start of BMMNC injection for a total of 30 minutes. Then, GFP-positive cell number was counted in each 1-minute effluent sample using a hemocytometer (enhanced Niebauer type) under fluorescent microscopy (Nikon). The difference between the injected BMMNC number and the GFP-positive cell number in the coronary effluent was regarded as the number of BMMNC retained in the myocardium. In this cell injection system, when cells were injected without hanging the heart, >99% of cells were viable in the effluent (analyzed by trypan-blue staining).

Antibody inhibition

Additional sets of hearts underwent I/R as just described and were then administered either monoclonal antibodies against P-selectin (BD Pharmingen; 150 μg/kg, P-selectin group), ICAM-1 (eBioscience; 200 μg/kg, ICAM-1 group) or VCAM-1 (eBioscience; 200 μg/kg, VCAM-1 group) via the aortic cannula ($n = 6$ in each group). Subsequently, 1×10^6 GFP-positive BMMNC were injected and the number of retained BMMNC was estimated as previously noted. Justification of antibody dose is explained in the Discussion section.

Characterization of retained BMMNC

At 30 minutes after cell injection, the hearts in the I/R groups ($n = 6$) were minced and digested with 1.2 U/ml dispase (Worthington), 5 mg/ml collagenase IV (Worthington) and 5 mmol/liter $CaCl_2$ at 37°C for 45 minutes.[16,17] Cell suspension, containing GFP-positive retained cells, were purified using Percoll gradient and labeled with the same antibodies as noted previously.

Endothelial expression of adhesion molecules (immunofluorescence)

Additional hearts were perfused for 20 minutes only ($n = 3$) or 20 minutes followed by I/R ($n = 3$), and then frozen. Cryosections were labeled with anti–P-selectin, anti–ICAM-1 and anti–VCAM-1 antibodies with nuclei counterstaining using with 4',6-diamidino-2-phenylindole (DAPI) to compare hearts with vs without I/R using confocal microscopy (LSM500; Zeiss).

Histologic assessment of retained BMMNC in recipient hearts

Additional heart samples were prepared for histologic studies. After BMMNC injection with ($n = 3$) or without ($n = 3$) I/R, 4%

paraformaldehyde was injected into hearts from the aortic cannula, which were then frozen. Cryosections were labeled with anti-platelet endothelial adhesion molecule (PECAM)-1 antibody (BD Pharmingen) with DAPI counterstaining and were examined by confocal microscopy.

Statistical analysis

All values are expressed as mean ± SEM. The retention efficiency and coronary flow was compared using 1- and 2-way analysis of variance (ANOVA), respectively, followed by Bonferroni's test. The proportion positive for PSGL-1, CD18 or Sca-1 before injection and after retention was compared using the unpaired *t*-test. $p < 0.05$ was considered statistically significant.

Results

Characterization of mononuclear BMMNC derived from GFP-transgenic mice

Each GFP-transgenic mouse yielded 20 to 30 million BMMNC. Almost all BMMNC had a round morphology showing an intense GFP signal under fluorescent microscopy (data not shown). Among the viable BMMNC (>97% of total), 98.1 ± 0.3% were positive for GFP. GFP-positive viable BMMNC expressed PSGL-1 in 49.3 ± 3.5%, CD18 in 57.5 ± 6.2%, Sca-1 in 6.4 ± 0.5%, CD45 in 95.4 ± 1.3%, CD34 in 0.9 ± 0.2% and c-kit in 0.4 ± 0.1%.

Endothelial expression of adhesion molecules

Immunoconfocal microscopy showed that P-selectin was rarely expressed in the normal hearts (Figure 1A), but largely upregulated after I/R (Figure 1B). In contrast, although ICAM was expressed in the normal hearts at a low level, ICAM-1 expression was not upregulated after I/R (Figure 1C and D). VCAM-1 was rarely expressed regardless of I/R (Figure 1D and E).

Retention efficiency of BMMNC

Frequency of BMMNC retention was assessed by counting the GFP-positive cell number in the coronary effluent. Almost all cells found in the effluent were GFP-positive. Over 95% of flushed-out BMMNC in the effluent occurred within 1 minute after injection. Retention efficiency of BMMNC in the Normal group was estimated to be 13.3 ± 1.2% of the total BMMNC injected (Figure 2). In contrast, prior I/R induction (I/R group) increased retention efficiency to 36.5 ± 1.6%. This increased retention was diminished by antibody inhibition for P-selectin (8.3 ± 0.8%), but not for ICAM-1 (39.6 ± 3.3%) or VCAM-1 (43.9 ± 2.9%).

Change in coronary flow

Coronary flow prior to cell injection was significantly reduced by I/R (I/R, P-selectin, ICAM-1 and VCAM-1 groups) compared with the Normal group (Table 1). BMMNC injection did not affect coronary flow in any of the groups until 20 minutes.

Distribution of retained BMMNC after intracoronary injection

Semi-quantitative frequency and morphologic change of retained BMMNC was assessed under confocal microscopy. GFP-positive cells were widely disseminated in the entire myocardium of the Normal group (Figure 3A). Also, much larger numbers of disseminated GFP-positive cells were detected in the I/R group (Figure 3B). Furthermore, PECAM-1/DAPI staining showed that a considerable number of retained GFP-positive BMMNC appeared to have extravasated, being localized outside the PECAM-1–positive vasculatures with a marked morphologic change suggesting transendothelial migration, within a minute after cell injection, in both normal and I/R hearts (Figure 3C). In contrast, a very small number of GFP-positive cells retained the round morphology and appeared to adhere to the PECAM-1–positive endothelium (Figure 3C). Histologic observations suggested no plugging (aggregation) of donor cells in any of the sizes of vasculatures in any areas in either group.

Expression of PSGL-1, CD18 and Sca-1 in retained BMMNC

The GFP-positive BMMNC retained into I/R hearts were collected by enzymatic digestion, and characterized by flow cytometry. The GFP-positive cell proportion was 6.8 ± 3.2% of all cells collected from the hearts. The proportion of PSGL-1–positive cells in the BMMNC before injection was 49.3 ± 3.5% (Figure 4A), but this proportion was much reduced among retained BMMNC (1.3 ± 0.4%; Figure 4B and C). Conversely, the ratio of CD18-positive cells among retained BMMNC (57.5 ± 6.2%; Figure 4E) was similar to that before injection (59.6 ± 1.8%; Figure 4D and F). The proportion of Sca-1–positive cells was significantly greater among retained BMMNC (17.5 ± 0.9%; Figure 4H and I) compared with BMMNC before injection (6.4 ± 0.5%; Figure 4G). PSGL-1 expression in Sca-1–positive BMMNC before injection (43.6 ± 2.1%) was similar to that in the entire BMMNC population before injection.

Discussion

Quantitative study of initial retention of donor cells after intracoronary injection in vivo is not possible in small rodents due to the lack of a reproducible model for selective injection into the coronary arteries. As an alternative, in this investigation we used ex vivo crystalloid perfusion of mouse hearts. Most importantly, this model enabled consistent intracoronary cell injection under simplified, controlled coronary perfusion, allowing quantitative investigations of BMMNC retention. Furthermore, this was particularly use-